NPL
National Physical Laboratory

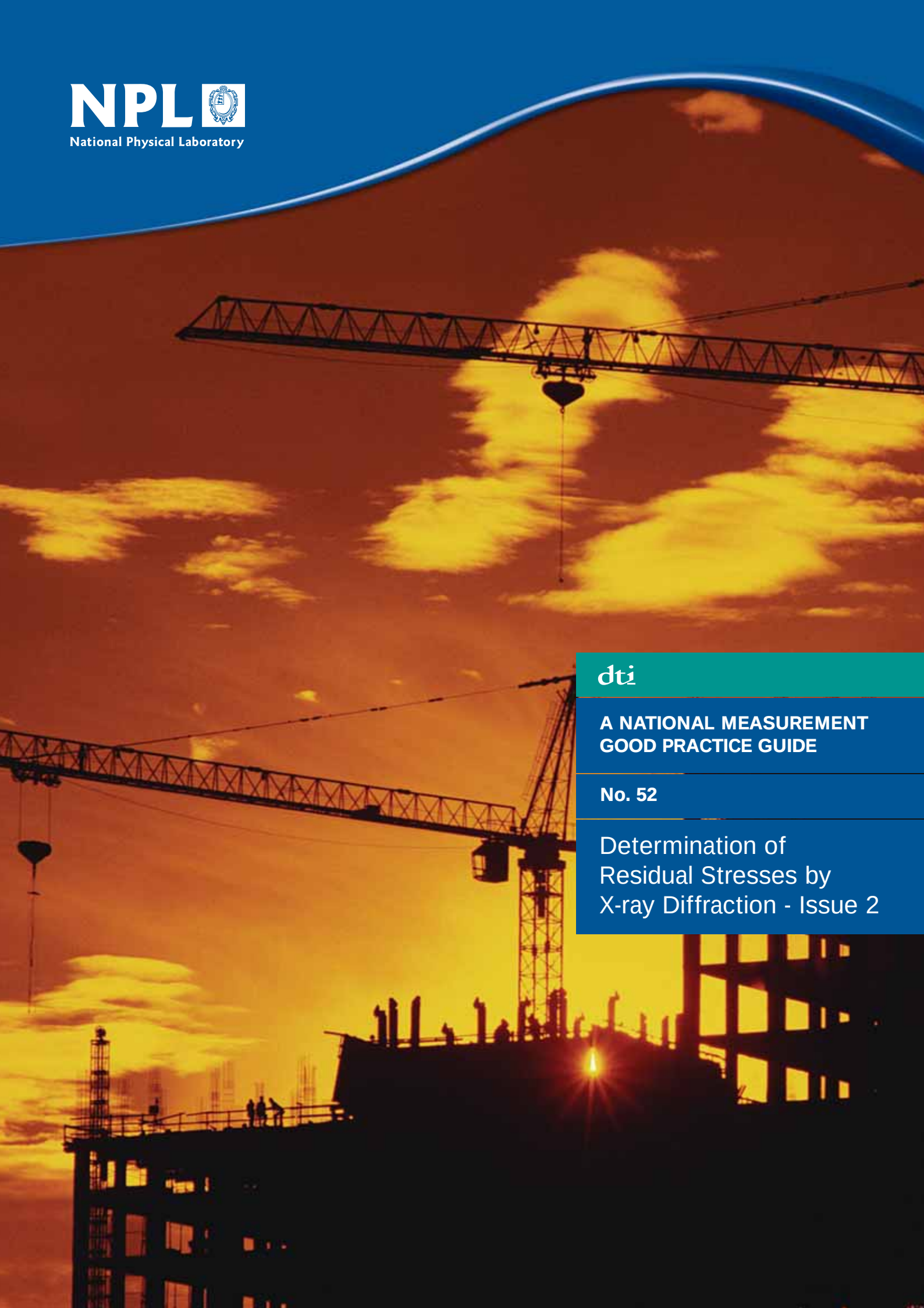

dti

A NATIONAL MEASUREMENT GOOD PRACTICE GUIDE

No. 52

Determination of Residual Stresses by X-ray Diffraction - Issue 2

dti

The DTI drives our ambition of 'prosperity for all' by working to create the best environment for business success in the UK. We help people and companies become more productive by promoting enterprise, innovation and creativity.

We champion UK business at home and abroad. We invest heavily in world-class science and technology. We protect the rights of working people and consumers. And we stand up for fair and open markets in the UK, Europe and the world.

This Guide was developed by the National Physical Laboratory on behalf of the NMS.

Measurement Good Practice Guide No. 52

Determination of Residual Stresses by X-ray Diffraction – Issue 2

M.E. Fitzpatrick[1], A.T. Fry[2], P. Holdway[3],
F.A. Kandil[2], J. Shackleton[4] and L. Suominen[5]
[1] Open University, [2] National Physical Laboratory, [3] QinetiQ,
[4] Manchester Materials Science Centre, [5] Stresstech Oy

Abstract:

This Guide is applicable to X-ray stress measurements on crystalline materials. There is currently no published standard for the measurement of residual stress by XRD. This Guide has been developed therefore as a source of information and advice on the technique. It is based on results from three UK inter-comparison exercises, detailed parameter investigations and discussions and input from XRD experts. The information is presented in separate sections which discuss the fundamental background of X-ray diffraction techniques, the different types of equipment that can be used, practical issues relating to the specimen, the measurement procedure itself and recommendations on how and what to record and report. The appendices provide further information on uncertainty evaluation and some recommendations regarding the data analysis techniques that are available. Where appropriate key points are highlighted in the text and summarised at the end of the document.

This second issue includes a new section on depth profiling, additional examples of uncertainty evaluation and recommendations regarding X-ray elastic constants and data presentation.

ISSN 1744-3911

September 2005

National Physical Laboratory
Teddington, Middlesex, United Kingdom, TW11 0LW
Website: www.npl.co.uk

Acknowledgements

This Guide has been produced as a deliverable in MPP8.5 – a *Measurements for Processability and Performance of Materials* project on the measurement of residual stress in components. The MPP programme was sponsored by the Engineering Industries Directorate of the Department of Trade and Industry. The advice and guidance from the programme's Industrial Advisory Group and XRD Focus Group are gratefully acknowledged.

The authors would like to acknowledge important contributions to this work from Jerry Lord, the enthusiasm of the XRD Focus Group established for this project and all participants of the XRD Round Robin exercises.

For further information on X-ray diffraction or *Materials Measurement* contact Tony Fry or the Materials Enquiry Point at the National Physical Laboratory:

Tony Fry
Tel: 020 8943 6220
Fax: 020 8943 6772
E-mail: tony.fry@npl.co.uk

Materials Enquiry Point
Tel: 020 8943 6701
Fax: 020 8943 7160
E-mail: materials@npl.co.uk

Contents

1 Introduction

In measuring residual stress using X-ray diffraction (XRD), the **strain** in the crystal lattice is measured and the associated **residual stress** is determined from the elastic constants assuming a linear elastic distortion of the appropriate crystal lattice plane. Since X-rays impinge over an area on the sample, many grains and crystals will contribute to the measurement. The exact number is dependent on the grain size and beam geometry. Although the measurement is considered to be near surface, X-rays do penetrate some distance into the material: the penetration depth is dependent on the anode, material and angle of incidence. Hence the measured strain is essentially the average over a few microns depth under the surface of the specimen.

At the time of publishing there are no published standards for the measurement of residual stress by XRD. The first issue of this guide was used to provide UK input into the European Standard being prepared by CEN TC 138/WG 10 "X-ray Diffraction". This second issue of the Measurement Good Practice Guide has been developed based on continued work from inter-comparison exercises, detailed parameter investigations and discussions conducted with XRD experts within Focus Groups to offer additional advice on good measurement practice.

This document contains additional advice and examples relating to depth profiling and uncertainty evaluation with regards to XRD measurements for the evaluation of residual stress in components. It is broken down into sections which discuss the fundamental background of X-ray diffraction techniques, the different types of equipment that can be used, practical issues relating to the specimen, the recommended measurement procedure and recommendations on how and what to record and report. The appendices provide further information on uncertainty evaluation and some recommendations regarding the data analysis techniques that are available.

2 Scope

This Measurement Good Practice Guide describes a recommended practice for measuring residual strains using X-ray diffraction. The method is non-destructive and is applicable to crystalline materials with a relatively small or fine grain size. The material may be metallic or ceramic, provided that a diffraction peak of suitable intensity, and free of interference from neighbouring peaks, can be produced.

The recommendations are meant for stress analysis where only the ***peak shift*** is determined. If a full triaxial analysis of stress is performed, using a stress-free reference, then the absolute peak location has to be determined. However, such an analysis is beyond the scope of this Guide, which assumes that measurements are made with the assumption that the stress normal to the surface is zero i.e. **plane stress conditions**, and so a full triaxial analysis is not required.

If measurements are performed which are outside of the scope of this document then the user should be aware that additional complexities are likely to occur, and extreme caution should be exercised with regards to experimental procedure and subsequent data analysis and interpretation.

In all instances it is recommended that the user consult with the manufacturer's guide in association with this document.

During the measurement, the user is responsible for adhering to the relevant safety procedures for ionising radiations imposed by Law.

3 Definitions

Normal Stress

Normal stress is defined as the stress acting normal to the surface of a plane; the plane on which these stresses are acting is usually denoted by subscripts. For example consider the general case as shown in Figure 3.1, where stresses acting normal to the faces of an elemental cube are identified by the subscripts that also identify the direction in which the stress acts,

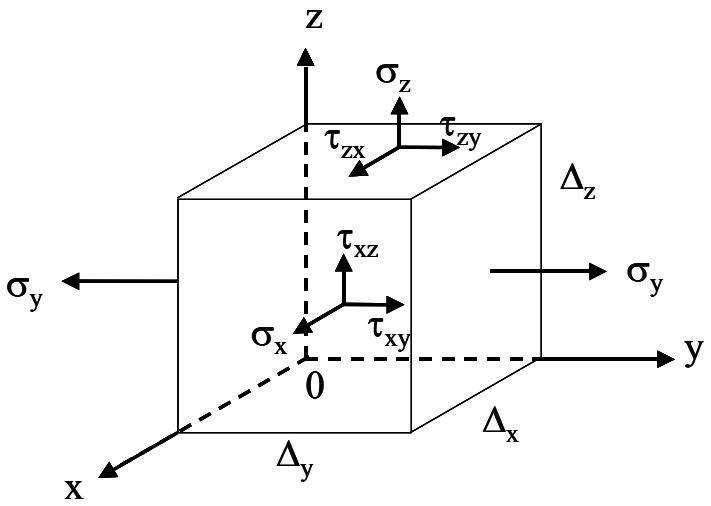

Figure 3.1 Stresses acting on an elemental unit cube.

e.g. σ_x is the normal stress acting in the x direction. Since σ_x is a normal stress it must act on the plane perpendicular to the x direction. The convention used is that positive values of normal stress denote tensile stress, and negative values denote a compressive stress.

Shear Stress

A shear stress acts perpendicular to the plane on which the normal stress is acting. Two subscripts are used to define the shear stress, the first denotes the plane on which the shear stress is acting and the second denotes the direction in which the shear stress is acting. Since a plane is most easily defined by its normal, the first subscript refers to this. For example, τ_{zx} is the shear stress on the plane perpendicular to the z-axis in the direction of the x-axis. The sign convention for shear stress is shown in Figure 3.2, which follows Timoshenko's notation. That is, a shear stress is positive if it points in the positive direction on the positive face of a unit cube. It is negative if it points in the negative direction of a positive face. All of the shear stresses in (a) are positive shear stresses regardless of the type of normal stresses that are present, likewise all the shear stresses in (b) are negative shear stresses.

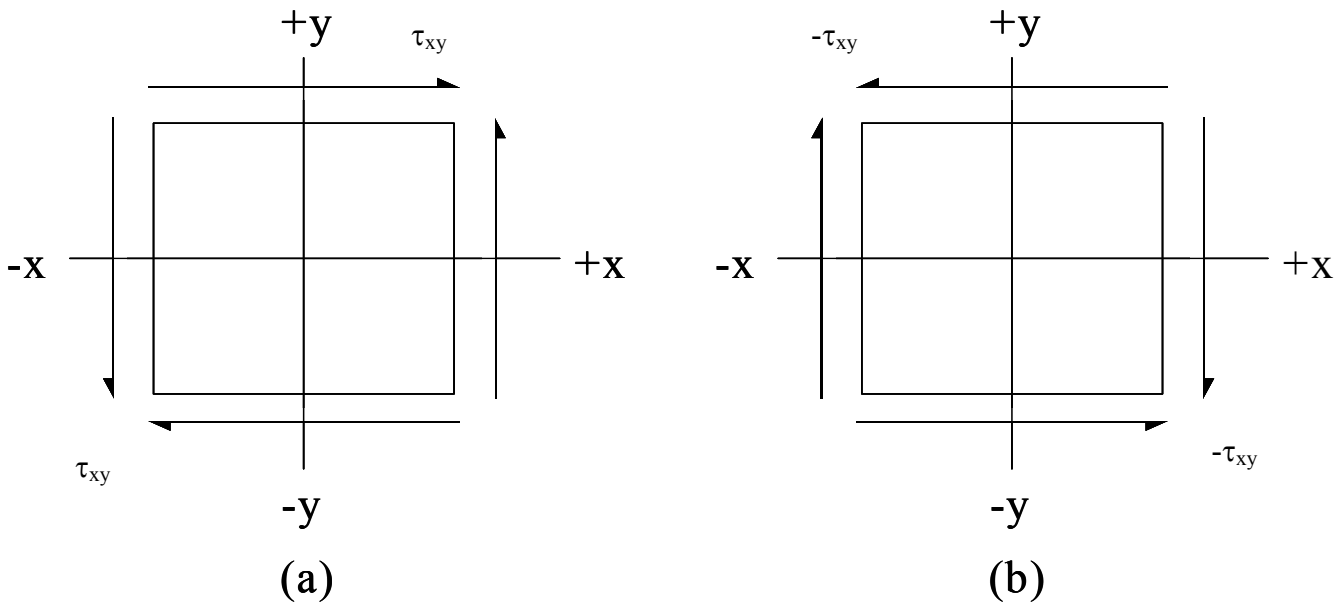

Figure 3.2 Sign convention for shear stress - (a) Positive, (b) negative.

Principal Stress

Principal stresses are those stresses that act on the 'principal planes'. For any state of stress it is possible to define a coordinate system, which has **axes perpendicular to the planes** on **which only normal stresses act** and on **which no shear stresses act.** These planes are referred to as the principal planes. In the case of two-dimensional plane stress there are two principal stresses σ_1 and σ_2. These occur perpendicular to each other, and by convention σ_1 is algebraically the largest. The directions along which the principal stresses act are referred to as the principal axes 1, 2 and 3. The specification of the principal stresses and their direction provides a convenient way of describing the stress state at a point.

4 Symbols

Symbol	Definition	Units
ARX	The anisotropy factor -this is a measure of the elastic anisotropy of a material. In the case of a non-cubic material or an elastic isotropic material the ARX value is 1	
a, b, c, α, β, γ	Lattice parameters (lattice constants) -parameters required to define the three vectors; **a**, **b**, **c**, which define the crystallographic axes of a unit cell and the angles (α, β, γ) between the vectors	Å
a_0, b_0, c_0	Strain free lattice parameters	Å
d	Inter-planar spacing (d-spacing) -the perpendicular distance between adjacent parallel crystallographic planes	Å
d_0	Strain free inter-planar spacing	Å
d_n	Inter-planar spacing of planes normal to the surface	Å
d_ψ	Inter-planar spacing of planes at an angle ψ to the surface	Å
E	Elastic modulus	GPa
E_{hkl}	Elastic modulus of the diffraction plane	GPa
G_x	Total intensity diffracted by a finite layer expressed as a fraction of the total diffracted intensity (see Ref. 2)	
{hkl}	Miller indices describing a family of crystalline planes	
I_0	Beam intensity	
L	Distance from the point of diffraction to a screen or detector	m
LPA	Lorentz-Polarization-Absorption factor	
n	An integer	
$S_{1\{hkl\}}$, $\frac{1}{2}S_{2\{hkl\}}$	X-ray elastic constants of the family of planes {hkl}	MPa^{-1}
χ (chi)	Angle of rotation in the plane normal to that containing omega and 2-theta about the axis of the incident beam.	°
$2\theta_{\phi\psi}$	Peak position in the direction of the measurement	°
ϕ (phi)	Angle between a fixed direction in the plane of the sample and the projection in that plane of the normal of the diffracting plane	°
ψ (psi)	Angle between the normal of the sample and the normal of the diffracting plane (bisecting the incident and diffracted beams)	°
$\varepsilon_{\phi\psi}$	Strain measured in the direction of measurement defined by the angles phi, psi	
ε_1, ε_2, ε_3	Principal strains acting in the principal directions	
ε_x	Strain measured in the X direction	
ε_y	Strain measured in the Y direction	
ε_z	Strain measured in the Z direction	
σ	Normal stress	MPa
σ_x	Stress in the X direction	MPa
σ_1, σ_2, σ_3	Principal stresses acting in the principal directions	MPa
σ_ϕ	Single stress acting in a chosen direction i.e. at an angle ϕ to σ_1	MPa
θ	Angular position of the diffraction lines according to Bragg's Law	°
ν	Poisson's ratio	
μ	Linear absorption coefficient	
τ	Normal shear stress	MPa
λ	Wavelength of the X-ray	Å
ω (omega)	Angular rotation about a reference point -the angular motion of the goniometer of the diffraction instrument in the scattering plane	°
1, 2, 3	Principal directions relevant to Cartesian co-ordinate axis	
x, y, z	Directions relevant to Cartesian co-ordinate axis	

5 Principles

The measurement of residual stress by X-ray diffraction (XRD) relies on the fundamental interactions between the wave front of the X-ray beam, and the crystal lattice. For further information regarding these interactions the reader is referred to Huygen's principle and Young's double slit experiments[1]. The basis of all XRD measurements is described in Bragg's Law, which is discussed below.

5.1 Bragg's Law

Consider a crystalline material made up of many crystals, where a crystal can be defined as *a solid composed of atoms arranged in a pattern periodic in three dimensions*[1]. These periodic planes of atoms can cause constructive and/or destructive interference patterns by diffraction. The nature of the interference depends on the inter-planar spacing d, and the wavelength of the incident radiation λ.

In 1912 W. L. Bragg (1890-1971) analysed some results from experiments conducted by the German physicist von Laue (1879-1960), in which a crystal of copper sulphate was placed in the path of an X-ray beam. A photographic plate was arranged to record the presence of any diffracted beams and a pattern of spots was formed on the photographic plate. Bragg deduced an expression for the conditions necessary for diffraction to occur in such a constructive manner.

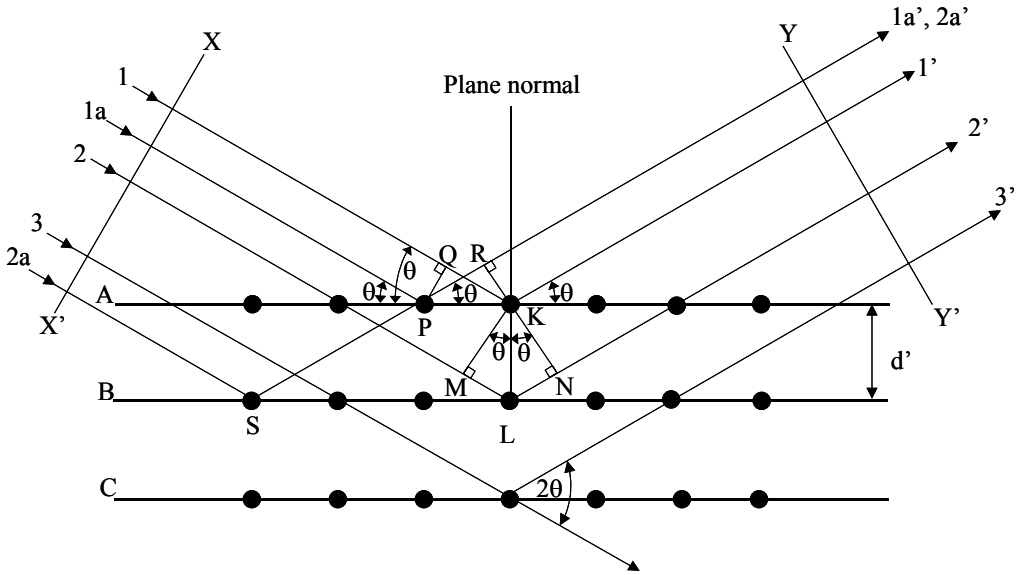

Figure 5.1 Diffraction of X-rays by a crystal lattice.

To explain Bragg's Law first consider a single plane of atoms, (row A in Figure 5.1). Ray **1** and **1a** strike atoms **K** and **P** in the first plane of atoms and are scattered in all directions. Only in directions **1'** and **1a'** are the scattered beams in phase with each other, and hence interfere constructively. Constructive interference is observed because the difference in their path length between the wave fronts XX' and YY' is equal to zero. That is

$$QK - PR = PK\cos\theta - PK\cos\theta = 0 \qquad \mathbf{1}$$

Any rays that are scattered by other atoms in the plane that are parallel to **1'** will also be in phase and thus add their contributions to the diffracted beam, thereby increasing the intensity. Now consider the condition necessary for constructive interference of rays scattered by atoms in different planes. Rays **1** and **2** are scattered by atoms **K** and **L**. The path difference for rays **1K1'** and **2L2'** can be expressed as

$$ML + LN = d'\sin\theta + d'\sin\theta \qquad \mathbf{2}$$

This term also defines the path difference for reinforcing rays scattered from atoms **S** and **P** in the direction shown in Figure 5.1, since in this direction there is no path difference between rays scattered by atoms **S** and **L** or **P** and **K**. Scattered rays **1'** and **2'** will be in phase only if the path difference is equal to a whole number *n* of wavelengths, that is if

$$n\lambda = 2d'\sin\theta \qquad \mathbf{3}$$

This is now commonly known as Bragg's Law and it forms the fundamental basis of X-ray diffraction theory.

5.2 Strain Measurement

To perform strain measurements the specimen is placed in the X-ray diffractometer, and it is exposed to an X-ray beam that interacts with the crystal lattice to cause diffraction patterns. By scanning through an arc of radius about the specimen the diffraction peaks can be located and the necessary calculations made, as detailed below. Further information regarding the different types of diffractometers and their constituent parts can be found in section 6.

It has been shown that there is a clear relationship between the diffraction pattern that is observed when X-rays are diffracted through crystal lattices and the distance between atomic planes (the inter-planar spacing) within the material. By altering the inter-planar spacing different diffraction patterns will be obtained. Changing the wavelength of the X-ray beam will also result in a different diffraction pattern. The inter-planar spacing of a material that is free from strain will produce a characteristic diffraction pattern for that material. When a material is strained, elongations and contractions are produced within the crystal lattice, which change the inter-planar spacing of the {hkl} lattice planes. This induced change in d will cause a shift in the diffraction pattern. By precise measurement of this shift, the change in the inter-planar spacing can be evaluated and thus the strain within the material deduced. To do this we need to establish mathematical relationships between the inter-planar spacing and the strain. The orthogonal coordinate systems used in the following explanations are defined in Figure 5.2.

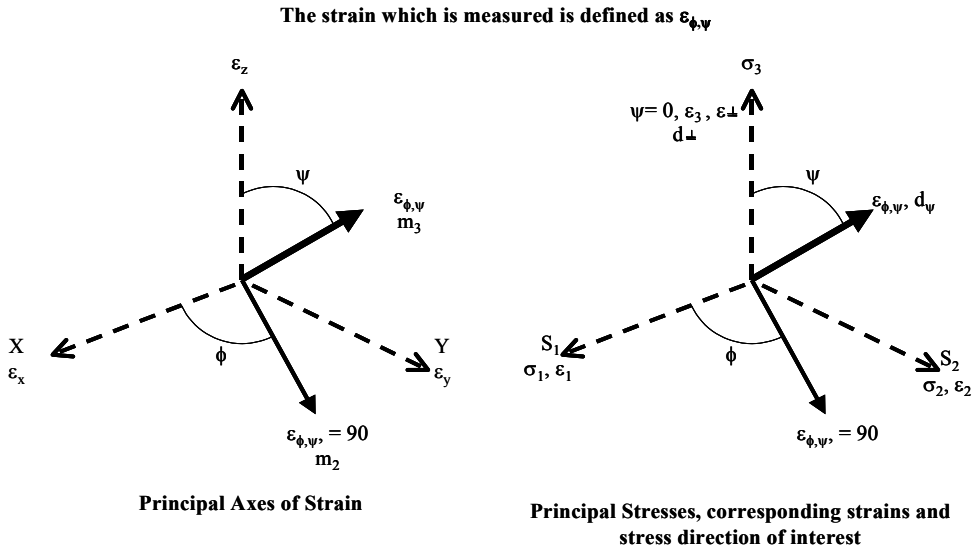

Figure 5.2 Co-ordinate system used for calculating surface strain and stresses. Note that ε_z and σ_3 are normal to the specimen surface

Let us assume that because the measurement is made within the surface, that $\sigma_3 = 0$. The strain ε_z however will not be equal to zero. The strain ε_z can be measured experimental by measuring the peak position 2θ, and solving equation 3 for a value of d_n. If we know the unstrained inter-planar spacing d_0 then;

$$\varepsilon_z = \frac{d_n - d_0}{d_0} \qquad 4$$

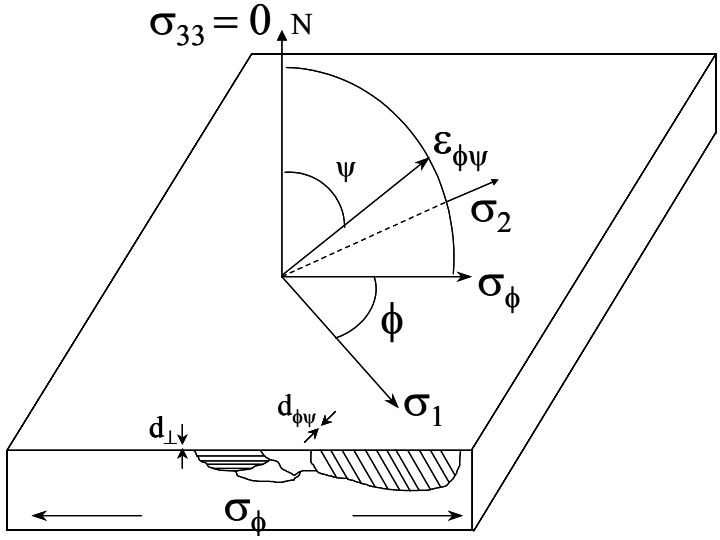

Figure 5.3 Schematic showing diffraction planes parallel to the surface and at an angle $\phi\psi$. Note σ_1 and σ_2 both lie in the plane of the specimen surface

Thus, the strain within the surface of the material can be measured by comparing the unstressed lattice inter-planar spacing with the strained inter-planar spacing. This, however, requires precise measurement of an unstrained sample of the material. Equation 4 gives the formula for measurements taken normal to the surface. By altering the tilt of the specimen

within the diffractometer, measurements of planes at an angle ψ can be made (see Figure 5.3) and thus the strains along that direction can be calculated using

$$\varepsilon_{\psi} = \frac{d_{\phi\psi} - d_0}{d_0} \qquad \textbf{5}$$

Figure 5.3 shows planes parallel to the surface of the material and planes at an angle ϕψ to the surface. This illustrates how planes that are at an angle to the surface are measured by tilting the specimen so that the planes are brought into a position where they will satisfy Bragg's Law.

5.3 Stress Determination

Whilst it is very useful to know the strains within the material, it is more useful to know the engineering stresses that are linked to these strains. From Hooke's law we know that

$$\sigma_y = E\varepsilon_y \qquad \textbf{6}$$

It is also well know that a tensile force producing a strain in the X-direction will produce not only a linear strain in that direction but also strains in the transverse directions. Assuming a state of plane stress exists, i.e. $\sigma_z = 0$, and that the stresses are biaxial, then the ratio of the transverse to longitudinal strains is Poisson's ratio, ν;

$$\varepsilon_x = \varepsilon_y = -\nu\varepsilon_z = \frac{-\nu\sigma_y}{E} \qquad \textbf{7}$$

If we assume that at the surface of the material, where the X-ray measurement can be considered to have been made (see section 5.4 on depth penetration), that $\sigma_z = 0$ then

$$\varepsilon_z = -\nu\left(\varepsilon_x + \varepsilon_y\right) = \frac{-\nu}{E}\left(\sigma_x + \sigma_y\right) \qquad \textbf{8}$$

Thus combining equations 4 and 8

$$\frac{d_n - d_0}{d_0} = -\frac{\nu}{E}\left(\sigma_x + \sigma_y\right) \qquad \textbf{9}$$

Equation 9 applies to a general case, where only the sum of the principal stresses can be obtained, and the precise value of d_0 is still required.

We wish to measure a single stress acting in some direction in the surface σ_ϕ. Elasticity theory for an isotropic solid shows that the strain along an inclined line (m_3 in Figure 5.2) is

$$\varepsilon_{\phi\psi} = \frac{1+\nu}{E}\left(\sigma_1 \cos^2\phi + \sigma_2 \sin^2\phi\right)\sin^2\psi - \frac{\nu}{E}\left(\sigma_1 + \sigma_2\right) \qquad \textbf{10}$$

If we consider the strains in terms of inter-planar spacing, and use the strains to evaluate the stresses, then it can be shown that

$$\sigma_\phi = \frac{E}{(1+\nu)\sin^2\psi}\left(\frac{d_\psi - d_n}{d_n}\right) \qquad 11$$

This equation allows us to calculate the stress in any chosen direction from the inter-planar spacings determined from two measurements, made in a plane normal to the surface and containing the direction of the stress to be measured.

The most commonly used method for stress determination is the $\sin^2\psi$ method. A number of XRD measurements are made at different psi tilts (see Figure 5.3). The inter-planar spacing, or 2-theta peak position, is measured and plotted as a curve similar to that shown in Figure 5.4.

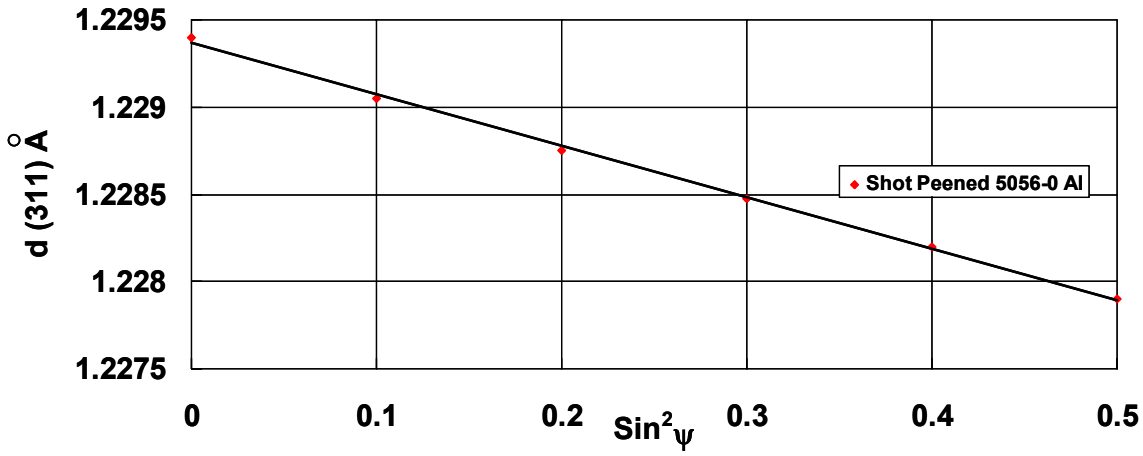

Linear dependence of d (311) upon $\sin^2\psi$ for shot peened 5056-0 aluminium

Prevey, P.S. "Metals Handbook: Ninth Edition," Vol. 10, ed. K. Mills, pp 380-392, Am. Soc. for Met., Metals Park, Ohio (1986)

Figure 5.4 Example of a d vs $\sin^2\psi$ plot

The stress can then be calculated from such a plot by calculating the gradient of the line and with basic knowledge of the elastic properties of the material. This assumes a zero stress at $d = d_n$, where d is the intercept on the y-axis when $\sin^2\psi = 0$, as shown in Figure 5.4.

Thus the stress is given by:

$$\sigma_\phi = \left(\frac{E}{1+\nu}\right)m \qquad 12$$

Where m is the gradient of the d vs. $\sin^2\psi$ curve.

For the full derivation of this solution the reader is referred to Ref. 1 and 2.

This is the basis of stress determination using X-ray diffraction. More complex solutions exist for non-ideal situations where, for example, psi splitting occurs (caused by the presence of shear stresses) or there is an inhomogeneous stress state within the material (Figure 5.5).

Such solutions are available within the literature and may be embedded within software packages.

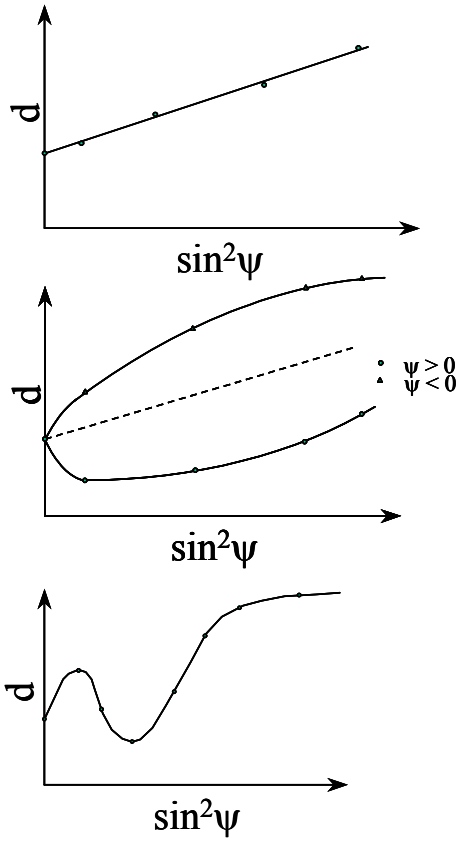

Regular d vs $\sin^2\psi$ behaviour with ε_{13} and ε_{23} being zero.

ψ-splitting - ε_{13} and/or ε_{23} are non-zero.

Oscillatory - indicating the presence of an inhomogeneous stress/strain state within the material usually due to Preferred orientation (texture).

Figure 5.5 Further examples of d vs $\sin^2\psi$ plots

Equation 11 assumes that the bulk modulus is the same as the modulus of the lattice plane being used for the measurement; this assumption is often not the case. A better method is to calculate or measure the elastic constants of a particular plane. To measure these constants a bending test must be performed in the diffractometer, and the reader is referred to ASTM E-1426-94 for further information. Most modern software will calculate the plane-specific constants for the analysis routines, but this may not be the case for all.

5.4 Depth of Penetration

Many metallic specimens strongly absorb X-rays, and because of this the intensity of the incident beam is greatly reduced in a very short distance below the surface. Consequently the majority of the diffracted beam originates from a thin surface layer, and hence the residual stress measurements correspond only to that layer of the material. This begs the question of what is the effective penetration depth of X-rays and to what depth in the material does the diffraction data truly apply? This is not a straightforward question to answer and is dependent on many factors that include the absorption coefficient of the material for a particular beam, and the beam dimensions on the specimen surface.

No precise answer can be given for the penetration depth. What is observed is that the intensity decreases exponentially with depth in the material. The rationale for this is as follows: the attenuation, loss in signal strength, is proportional to the distance travelled in a material, hence the contribution to the diffracted beam from layers, or planes, deeper down in

the material becomes less. Coupled with this is the fact that the diffracted beam still has to exit the material, thereby travelling through more material and suffering more attenuation.

The thickness (x) of the effective layer can be calculated, and is shown below in equation 13. The full derivation is presented in Ref. 2.

$$x = \frac{\ln\left[\dfrac{1}{1-G_x}\right]}{\mu\left[\dfrac{1}{\sin(\theta+\psi)}+\dfrac{1}{\sin(\theta-\psi)}\right]} \qquad \textbf{13}$$

Figures 5.6 shows the penetration depths vs. sin2ψ for materials commonly used for residual stress measurements. The difference in the effective layer thickness with ψ angles becomes of greater importance when the test specimen exhibits a steep stress gradient [3].

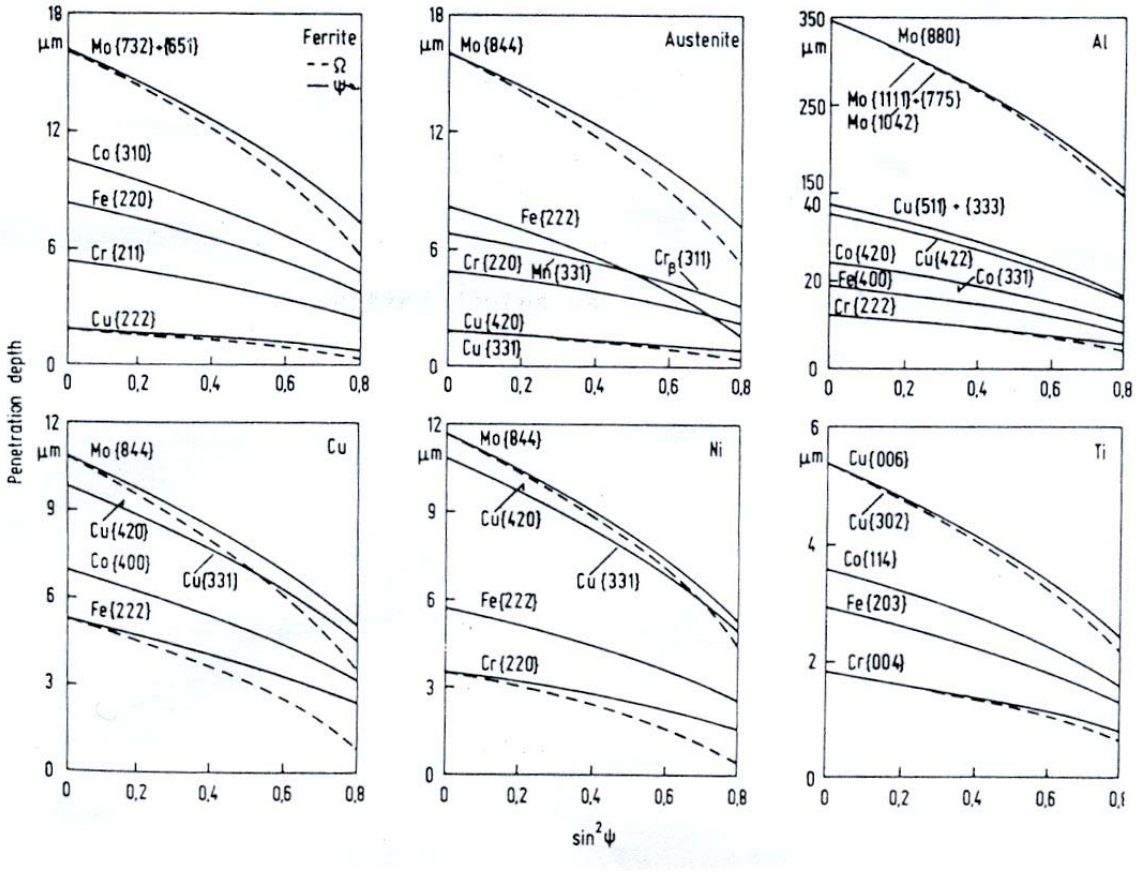

Figure 5.6 Penetration depths vs. $\sin^2\psi$ of different metals and radiations (After Ref. 5)

6 Apparatus

6.1 General

The diffractometers used for the measurement of residual stress are basically powder diffractometers, however they differ in the following ways:

- They can accommodate larger, heavier samples, as it is not usually desirable to cut small sections from large components.

- The maximum 2θ angle accessible to the instrument is large, typically 165° 2θ. (Most powder diffractometers cannot exceed 145° 2θ). Measurements can be made at very high 2θ values where the small changes in the d-spacings, due to strain, can be measured more precisely.

- A residual stress diffractometer has more axes of rotation than a standard powder diffractometer. This allows the sample to be "tilted" (rotated), in accordance with the requirements of the $\sin^2\psi$ method. For example, in residual stress diffractometers, both omega and 2-theta can be moved independently, i.e. they are "de-coupled". In a powder diffractometer omega is often fixed, mechanically, at half the value of 2-theta.

Residual stress diffractometers can be divided into two types (both of which have many variations):

- **Fixed, laboratory based systems,** where a sample is placed within the radiation enclosure of the instrument. These instruments are usually capable of other forms of X-ray diffraction analysis, for example, phase identification. The diffractometer in Figure 6.1 is a 'horizontal' goniometer, as are many laboratory based residual stress instruments.

Figure 6.1 Photograph of a typical laboratory system (courtesy of The Open University)

- **Portable systems**. These are designed specifically for stress analysis and are much smaller; they can often be carried easily. They can be taken to a large structure (for example, a bridge) and placed on the component of interest. Generally, they are much simpler in construction than laboratory based systems. They are designed to access small areas and awkward shaped components, such as gear teeth. (Figure 6.2)

Figure 6.2 Photograph of typical portable system (courtesy of Stresstech)

6.1.1 Diffraction Geometry

The Diffractometer angles used in residual stress analysis are:

- **2-theta (2θ)**
  The Bragg angle, this is the angle between the incident (transmitted) and diffracted X-ray beams.

- **Omega (ω)**
  The angle between the incident X-ray beam and the sample surface.
  Both omega and 2-theta lie in the same plane.

- **Phi (ϕ)**
  The angle of rotation of the sample about its surface normal.

- **Chi (χ)**
  Chi rotates in the plane normal to that containing omega and 2-theta. This angle is also sometimes (confusingly) referred to as ψ.

- **Psi (ψ)**
  Angles through which the sample is rotated, in the $\sin^2\psi$ method. We start at psi = 0, where omega is half of 2-theta and add (or subtract) successive psi offsets, for example, 10, 20, 30 and 40°.

These angles are illustrated in Figure 6.3, which shows the arrangement in a laboratory type goniometer measuring a large 2-theta angle, as used in residual stress analysis.

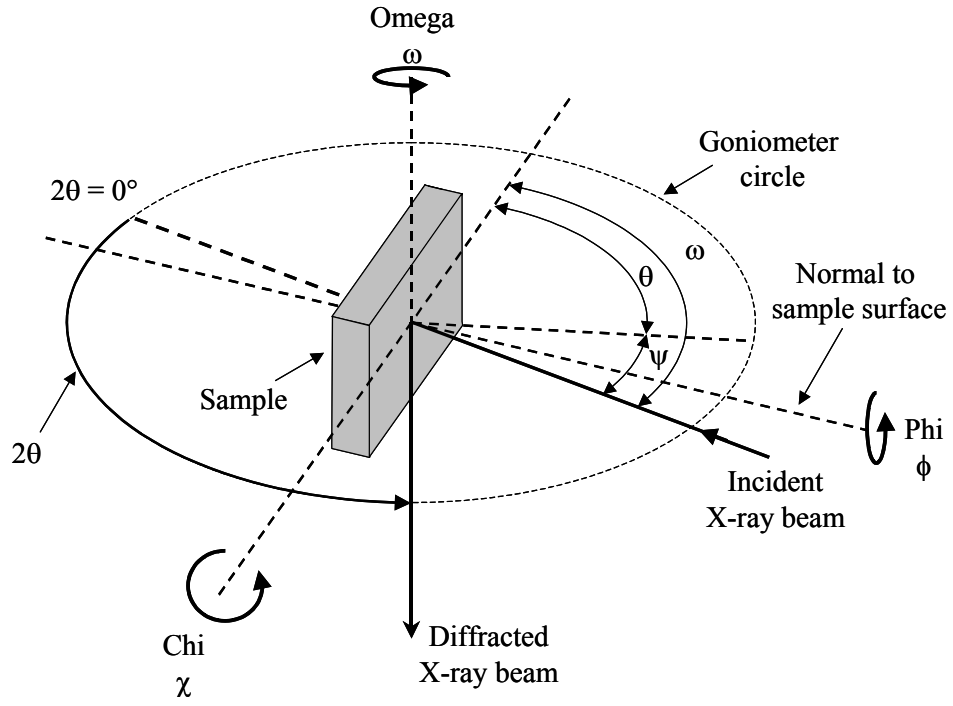

Figure 6.3 Angles and rotations used in residual stress measurement
(For a horizontal system with a positive psi offset.)

There are two methods of rotating the sample when residual stress is measured by the $\sin^2\psi$ technique:

- **The Omega Method**
  Here we rotate (tilt) the sample about the omega axis. Both omega and 2-theta are in the same plane. The values of psi are added, for positive psi (or subtracted, for negative psi), to theta. Most conventional powder diffractometers, with a de-coupled omega drive (where the omega and 2-theta axes are able to move independently) can make measurements using this method. The geometry is shown schematically in Figure 6.4. Omega is shown as equal to half 2-theta, i.e. in focused geometry (see Section 6.2.2 and Figures 6.10 and 6.11).

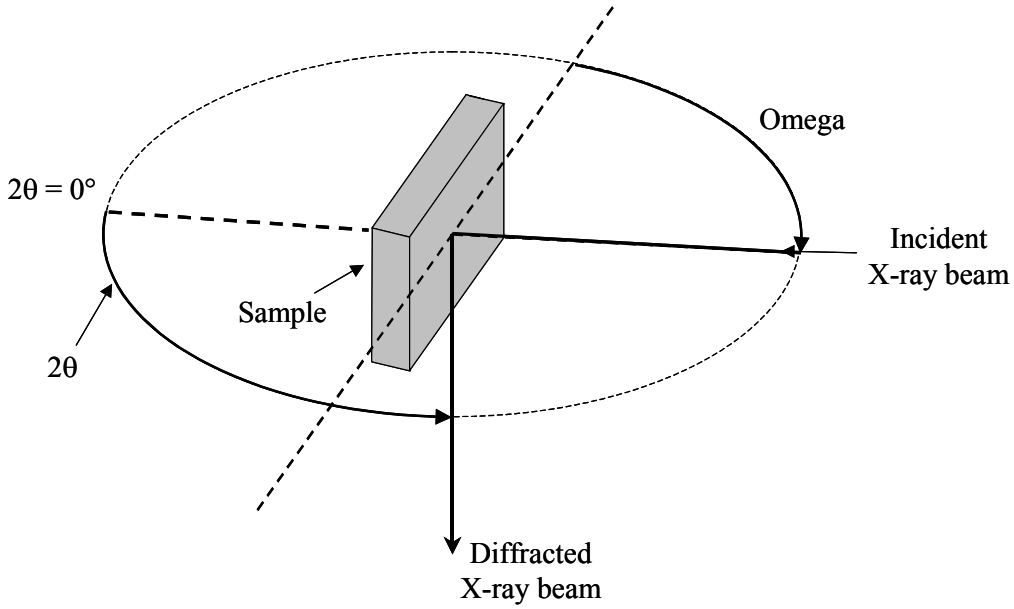

Figure 6.4 The omega method (Horizontal laboratory-type system shown from above)

- **The Chi Method**

  Figures 6.5a and 6.5b show the geometry of the chi method, which is also called the side inclination method. Here we rotate the sample about the chi axis, which is in a plane normal to that containing omega and 2-theta. Figure 6.5a shows the sample when chi = 0°. Figure 6.5b shows the sample rotated to a chi angle of 45°.

  Mechanically the chi method is a more complex method. Laboratory based diffractometers which use the chi method incorporate a special sample stage called an Eulerian (see Figure 6.1) cradle which enables the chi and phi rotations.

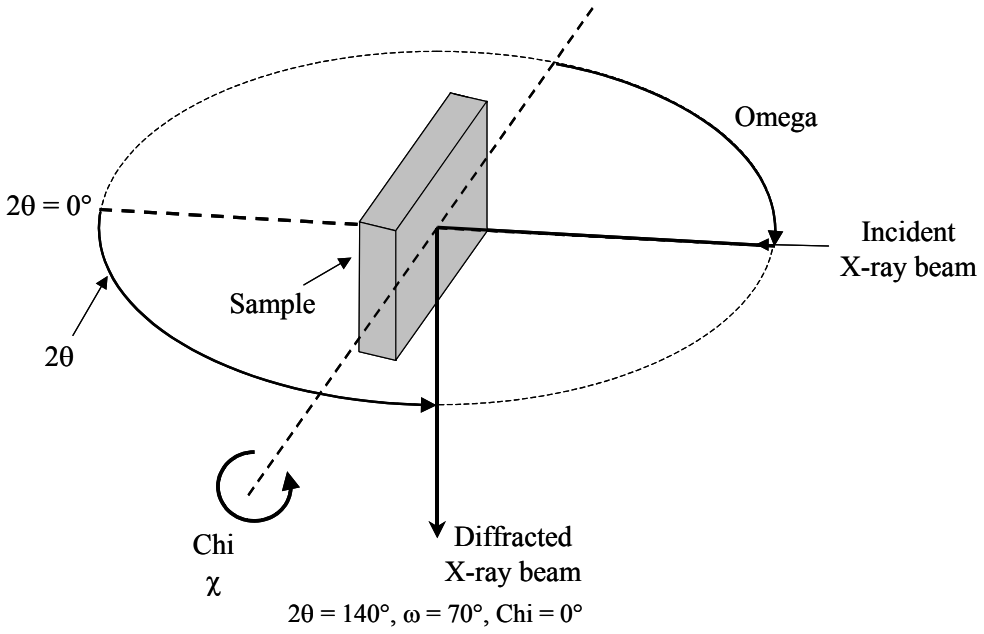

Figure 6.5a The chi method (Horizontal laboratory-type system shown from above)

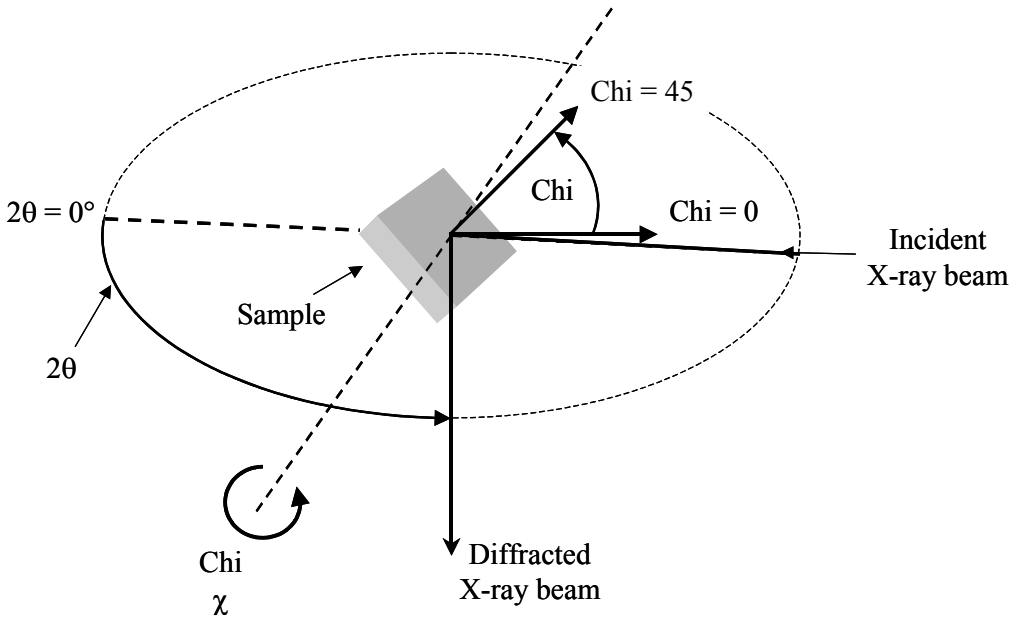

The normal to the sample surface is shown at Chi = 0° and Chi = 45°
(shown with 2θ = 140°, omega = 70° and Chi = 45°)

Figure 6.5b The chi method (Horizontal laboratory-type system shown from above)

6.1.2 Positive and Negative Psi Offsets

Figure 6.6 shows a sample with a positive psi offset, for the omega method, where psi has been added to theta. Figure 6.7 shows a negative psi offset where psi has been subtracted from theta.

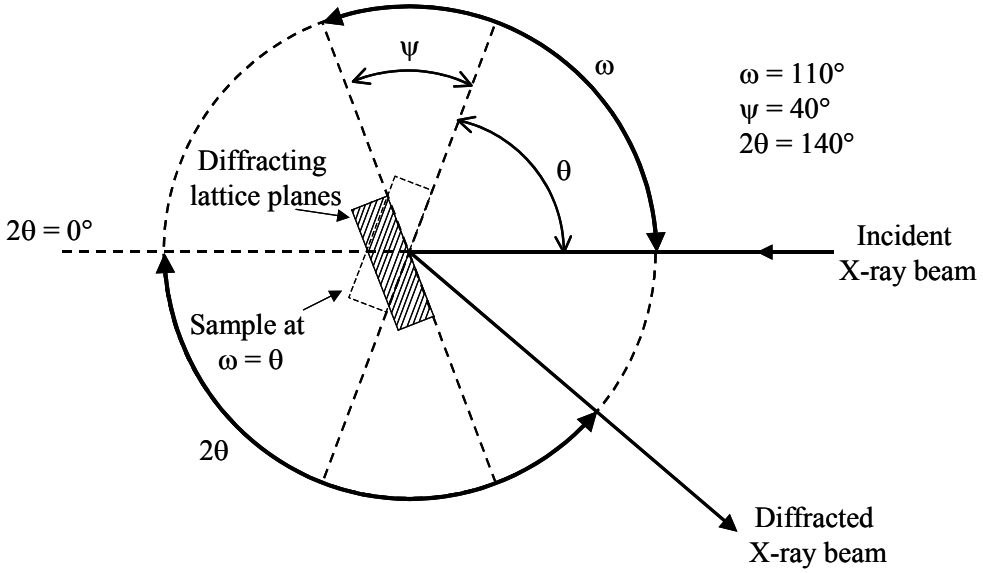

Figure 6.6 Positive psi offset ($\omega = \theta + \Psi$)

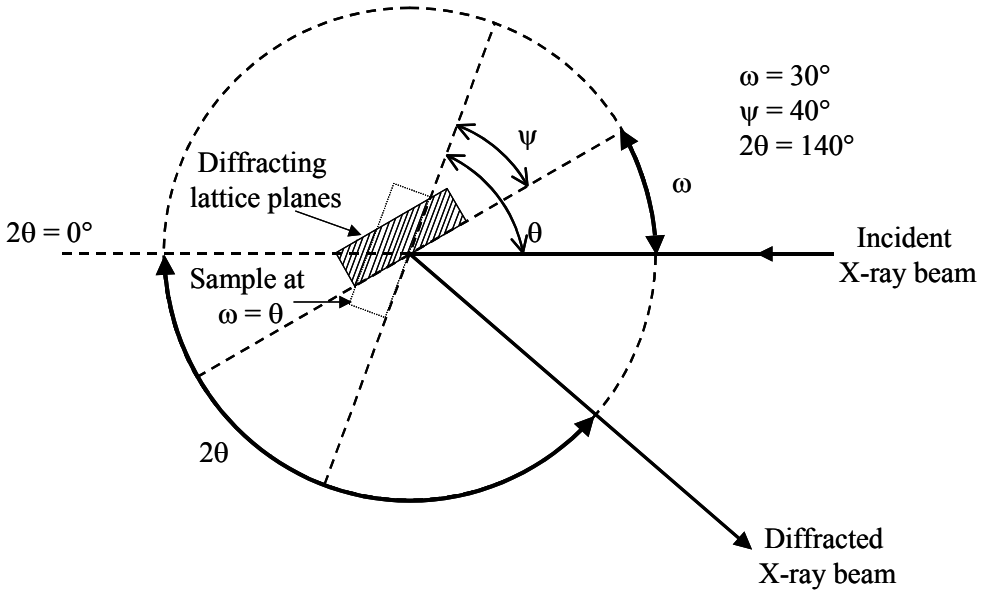

Figure 6.7 Negative psi offset ($\omega = \theta - \Psi$)

Note the small angle of incidence of the X-ray beam to the sample surface with the negative psi offset. Added to "defocusing" effects, which are discussed later, this makes the intensities from negative psi offsets lower than those from positive psi when the omega method is used. Negative psi offsets are used in the measurement of shear stresses. To avoid making measurements in negative psi, when using the omega method, we can rotate the sample

(around the phi axis) by 180° and measure positive psi. This is equivalent to a negative psi measurement without a phi rotation.

Obviously, defocusing effects are the same for positive and negative psi using the chi method, which is one of its advantages.

6.2 Major Components of Lab Based Stress Diffractometers

A schematic diagram of a laboratory-based diffractometer is shown below in Figure 6.8.

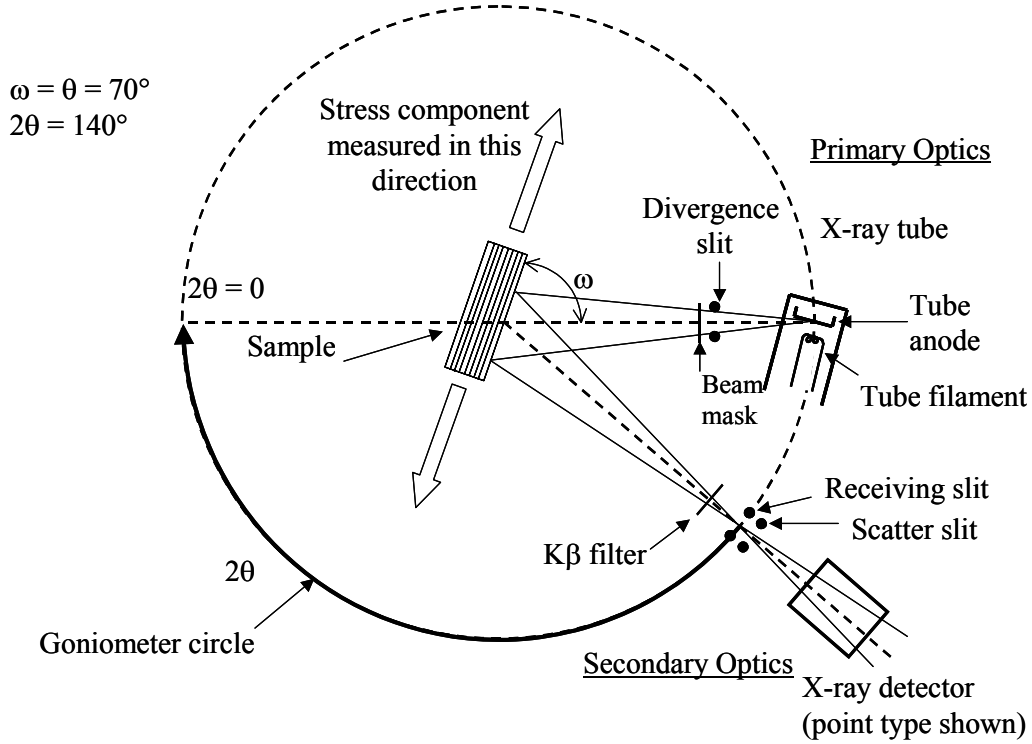

Figure 6.8 Schematic diagram showing major components of a horizontal laboratory-type focusing system

A *monochromatic source* of X-rays is required, which irradiates a *well-defined area* on the sample. The diffracted X-rays must then be detected with *adequate angular resolution.*

We will now consider how this is achieved by splitting the diffractometer into **three parts.**

- **The X-ray source**
  The X-ray tube.

- **The Primary Optics**
  These are the components between the X-ray source and the sample.

- **The Secondary Optics**
  These are the components between the sample and the detector.

6.2.1 The X-Ray Tube

All X-ray tubes work on the same principle. A focused beam of electrons is accelerated through a large potential difference (typically between 20 and 50 kV, supplied by a constant potential generator) and strikes a metal target or anode with considerable energy. X-rays are generated as a result. The detailed construction of X-ray tubes and their operation is given in Ref. 4. Most of the energy is dissipated as heat, only about 2% is converted into X-rays.

Laboratory-based systems have high-power X-ray tubes, usually about 2 kW. Portable systems, which rely on small cooling units that can be transported easily, have much lower rated tubes, usually about 200W. This is not of any practical significance as portable units have much shorter beam paths (usually about 10 cm as opposed to 20 cm) and consequently there is less air absorption.

If we plot the intensity of the X-rays generated against their wavelength, we obtain the spectrum shown in Figure 6.9.

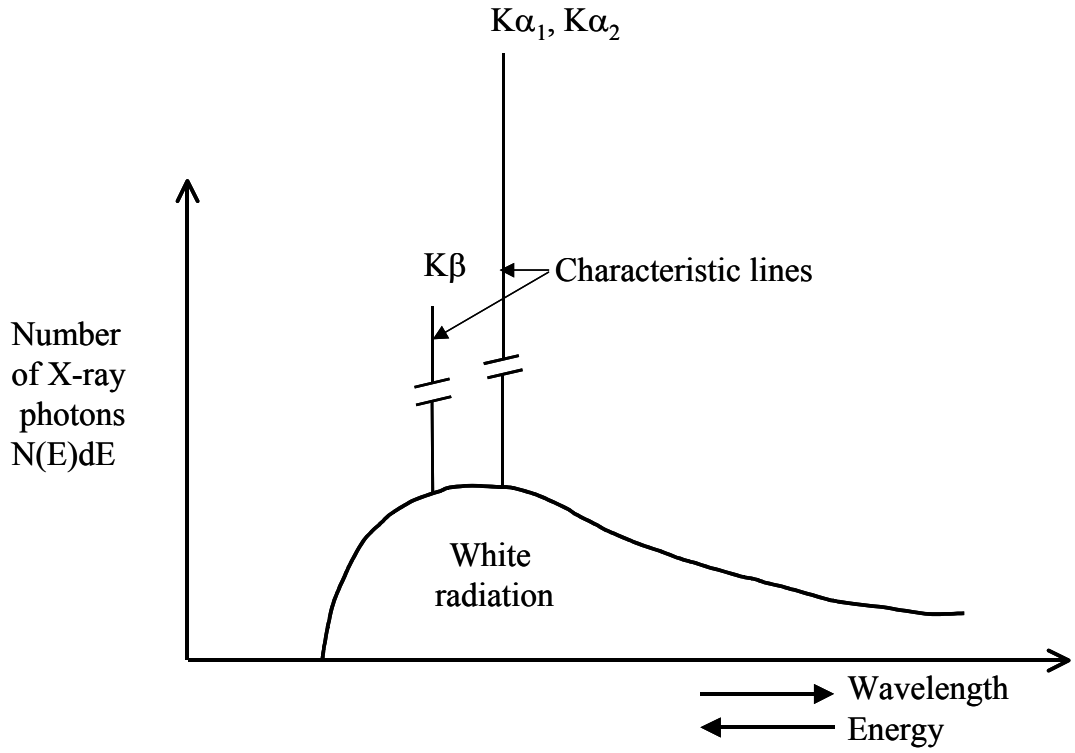

Figure 6.9 Schematic diagram of the X-ray spectrum from a tube

This X-ray spectrum can be divided into two parts:

6.2.1.1 Continuous Radiation

The smooth part of the curve is "continuous or white radiation," so-called as it is made up of many wavelengths, like white light, and is caused by the deceleration of the electrons inside the anode of the X-ray tube. As the continuous radiation is not monochromatic, it is undesirable. There are a variety of methods for reducing or removing it. The amount of

continuous radiation increases with the voltage applied to the X-ray tube and with the atomic number of the target.

6.2.1.2 Characteristic Radiation

Superimposed on the white radiation are a series of sharp, intense lines, called the characteristic lines. These have specific wavelengths and are observed when the accelerating voltage exceeds a critical value. The wavelength of the characteristic lines depends on the anode material, not on the accelerating voltage. For example, the wavelength of chromium K-α_1 is 2.290 Å and for iron K-α_1 it is 1.936 Å.

In X-ray diffraction, the K-α lines are used, as they are the most intense. The X-ray tube produces other characteristic lines, for example the K-β, which must be removed to achieve the goal of monochromatic radiation.

An X-ray tube should be selected with an anode material, which gives a suitable Bragg reflection (from our sample) at a sufficiently high 2-theta angle (ideally greater than 130° 2θ) to enable precise measurement of the *d*-spacing. Consequently, residual stress diffractometers usually have a selection of X-ray tubes available if they are to measure a wide range of materials. See Section 7, "*Radiation Selection*".

6.2.2 The Primary Optics

First we consider laboratory-based systems.

The X-ray beam from the tube is divergent, which is more suitable for conventional powder diffraction (often referred to as focused, or Bragg-Brentano geometry), where omega is always half of two-theta. In residual stress analysis however, omega or chi can take very different values and this destroys the usual focusing of the diffractometer.

For a divergent X-ray source, the X-ray beam no longer focuses on the detector slit; the focal point moves towards the sample. This is shown in an exaggerated form in Figure 6.10. When large psi offsets are used, a considerable amount of intensity is lost and the Bragg reflections appear broader. This effect is called *"defocusing"* and is observed in instruments which have a divergent primary beam, particularly with negative psi offsets (Figure 6.11).

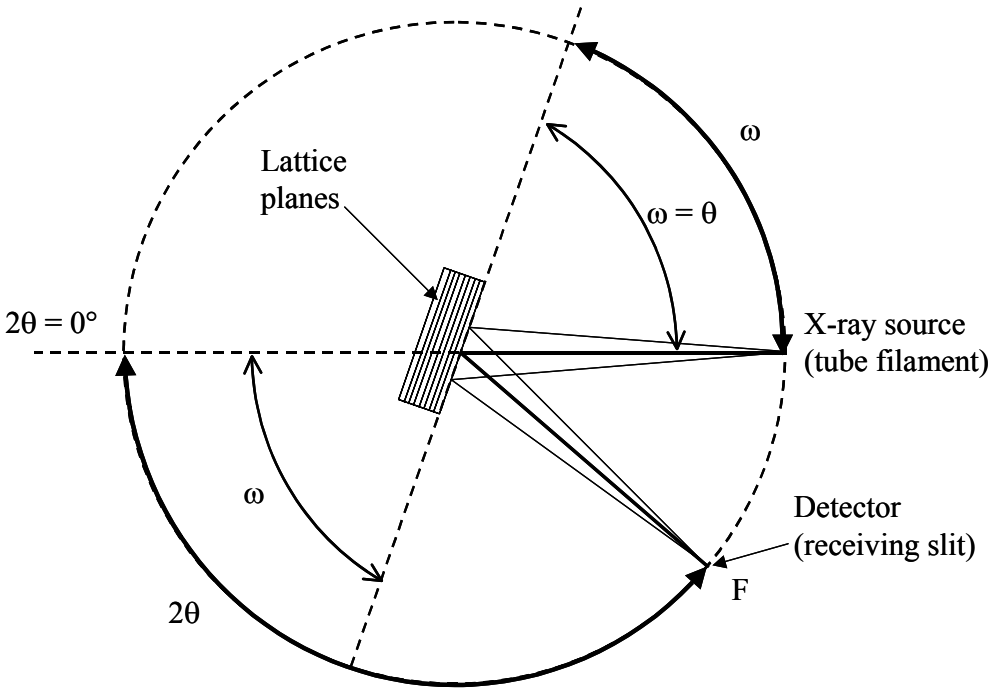

Figure 6.10 Focused geometry, Omega = θ (Horizontal system viewed from above)

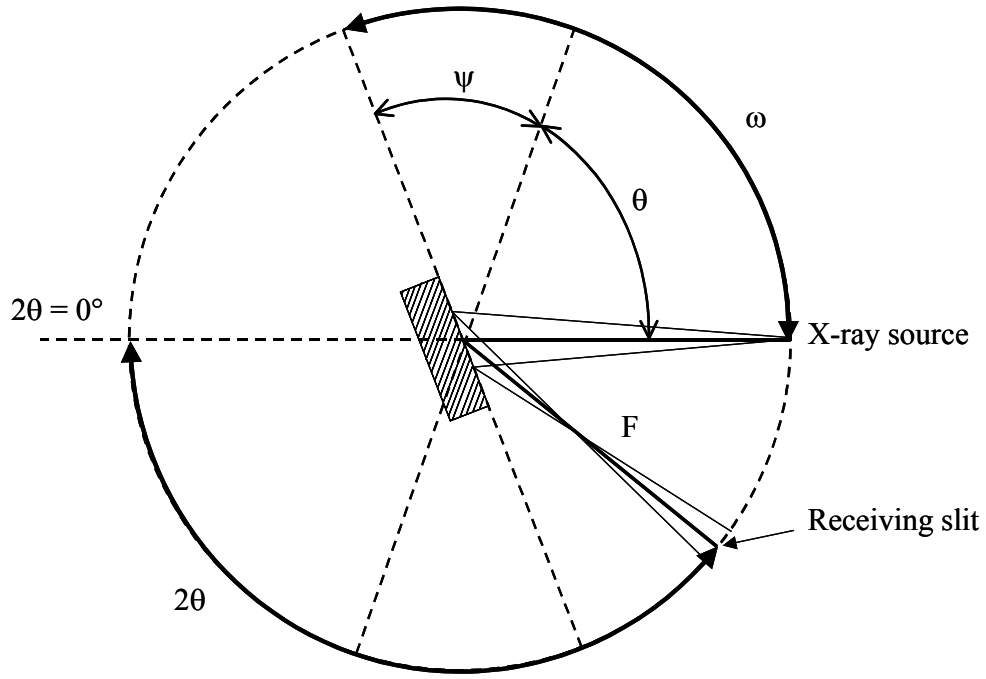

Figure 6.11 Defocused geometry, Omega = θ +Ψ (Horizontal system viewed from above)

Some residual stress diffractometers have devices to convert the divergent beam from the X-ray tube to a **parallel beam** and so greatly reduce defocusing. The parallel beam also makes the instrument less sensitive to sample positioning errors, although these errors are not eliminated.

6.2.2.1 Poly-Capillaries

A poly-capillary is an X-ray "light pipe" which is a bundle of optical fibres. The X-rays undergo total internal reflection inside the optical fibres. The divergent source is captured and converted into a largely parallel beam as shown in Figure 6.12.

Poly-capillaries have the advantage of working with all common X-ray wavelengths. They do not require re-alignment when the X-ray tube is changed. **The poly-capillary does not remove the K-β line or the continuous radiation.**

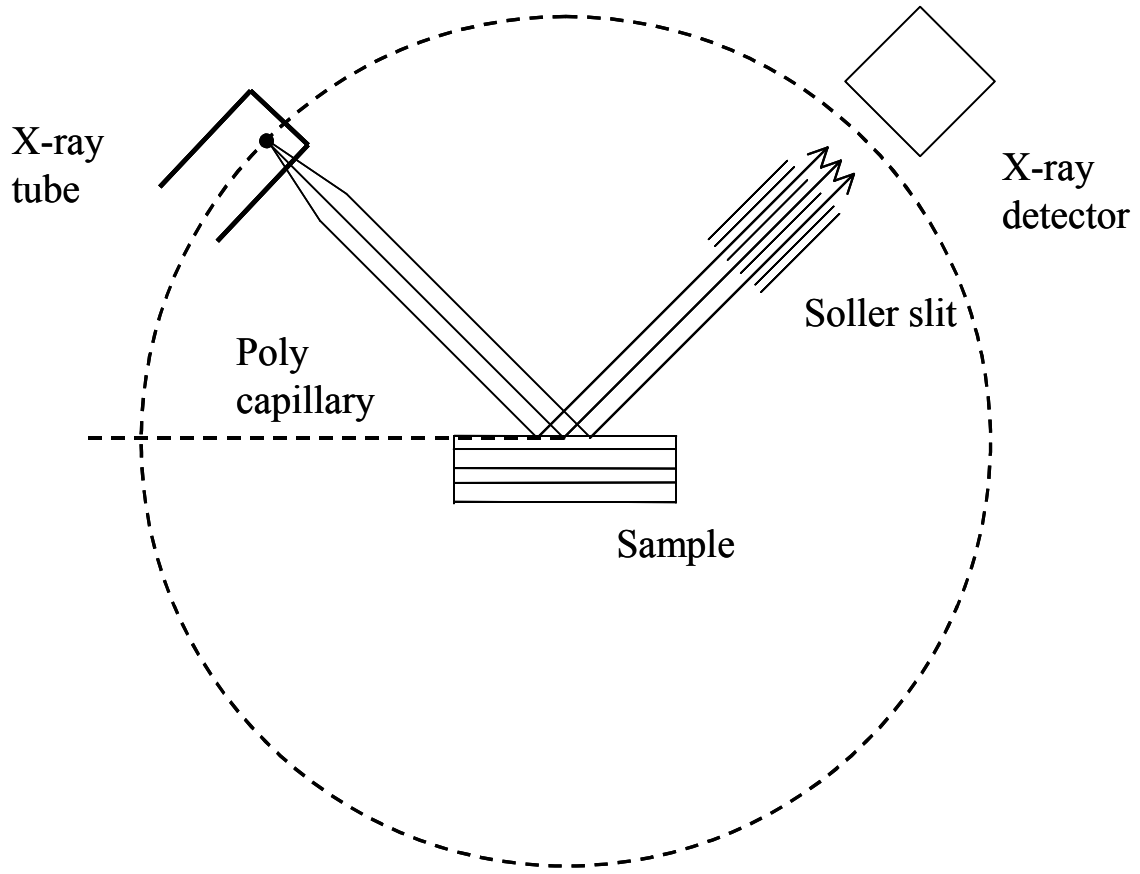

Figure 6.12 Poly-capillary, an X-ray "lightpipe", can be used with any wavelength

6.2.2.2 Mirrors

Mirrors are less common on residual stress machines as they are specific to a particular X-ray wavelength; usually copper K-α. An X-ray mirror is a shaped, synthetic crystal with a graded *d*-spacing which produces a very intense and parallel beam of X-rays, as shown in Figure 6.13.

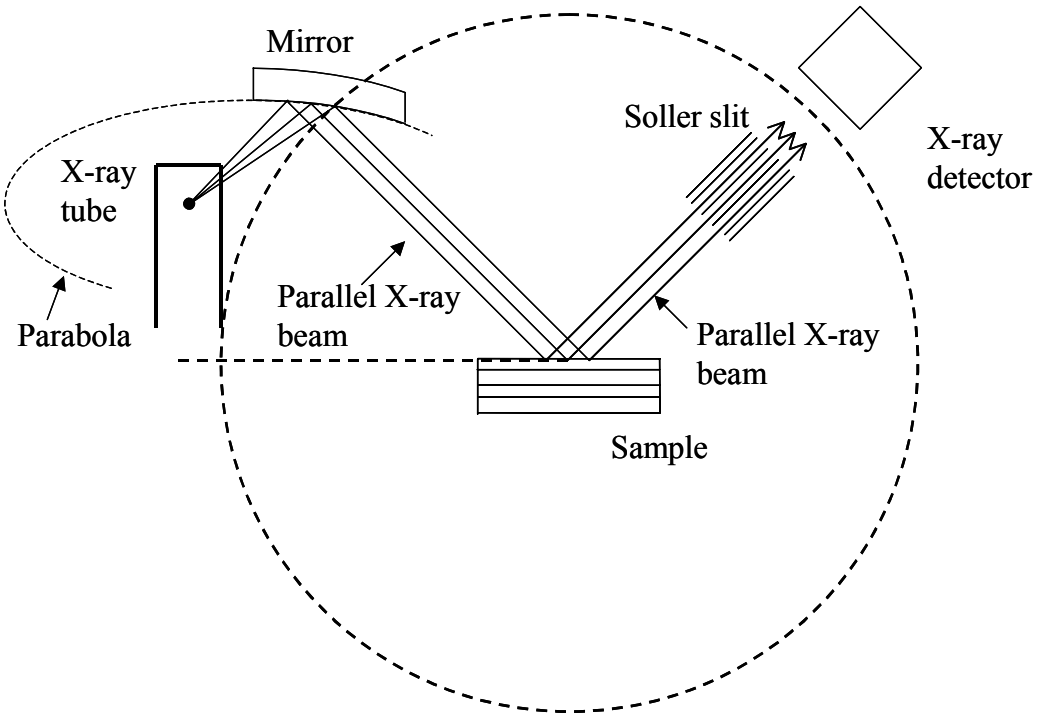

Figure 6.13 Schematic of an X-ray mirror

6.2.2.3 Slits

In most laboratory based systems the area of the sample which is irradiated is controlled by a slit in the primary optical path, called the divergence slit. Its aperture is measured in degrees: typical sizes are 1° and ½°. The divergence slit is combined with a mask, which limits the irradiated area laterally, as shown in figure 6.14.

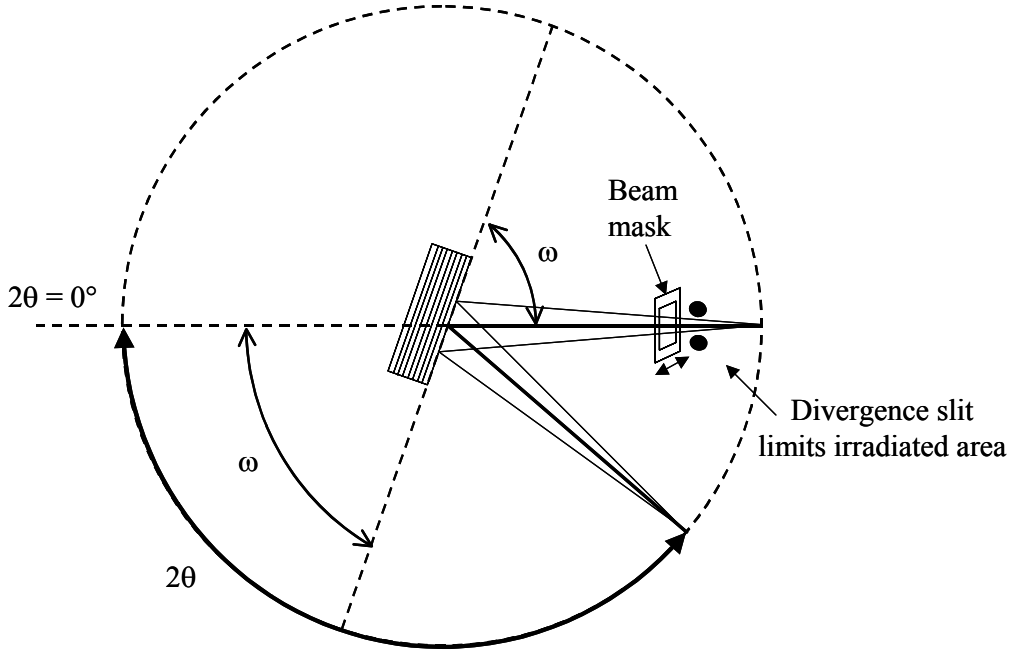

Figure 6.14 Primary divergence and beam mask-slit limits irradiated area with a divergent X-ray source (Horizontal system viewed from above)

6.2.3 Secondary Optics

6.2.3.1 K-β Filters

The K-β line can be removed by a filter, otherwise there will be two reflections from every set of lattice planes, one for the K-α and one for the K-β. The K-β filter is made from an element which preferentially absorbs the K-β wavelength, but is relatively transparent to the K-α. It has an absorption edge right on top of the K-β wavelength as shown in Figure 6.15.

The K-β filter is specific to the tube anode. The correct material for the beta filter can be determined easily as it is the element whose atomic number (Z) is one less that the anode material. For example, for a chromium anode X-ray tube the correct beta filter is vanadium, for an iron anode X-ray tube it is manganese.

The K-β filter is usually placed in the secondary optical path so that it absorbs some of the fluorescent radiation produced by the sample. The exception to this is when the sample contains the same element as the tube anode: here the K-β filter is placed on the primary side.

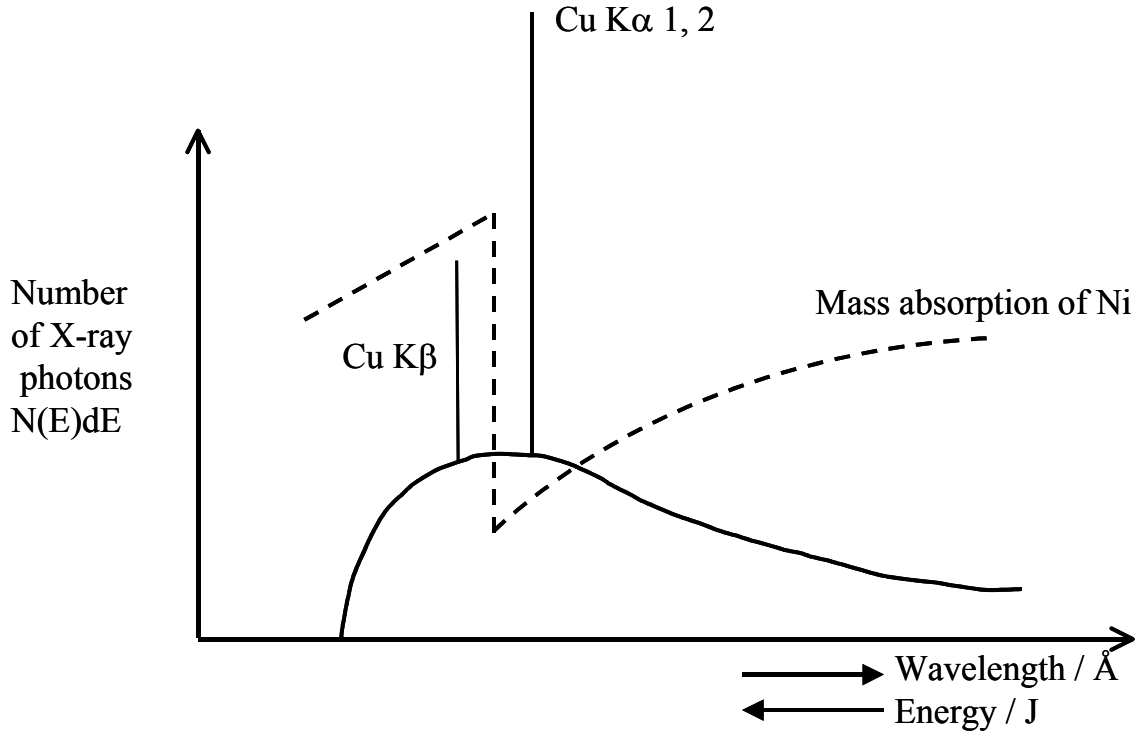

Figure 6.15 The K-β filter for copper radiation (The position of the Ni K absorption edge means that the Cu K-β line is absorbed but about 50% of the Cu K-a is transmitted).

6.2.3.2 Receiving Slits

The receiving slit is placed just in front of the detector and controls the angular resolution. Its aperture is measured in millimetres. A wide receiving slit will give poorer resolution but a higher count rate. Conversely, a narrow receiving slit will give better resolution but a much lower count rate.

For residual stress, the Bragg reflections are usually broad and there is significant defocusing at large psi angles, which increases the peak width still further. Consequently, **narrow receiving slits (less than 0.2 mm) are not suitable for residual stress analysis where we need a high-count rate to enable reliable peak fitting.** More useful choices are 0.3 and 0.4 mm.

6.2.3.3 Scatter Slits

The scatter slit is (usually) placed behind the receiving slit; it removes any unwanted radiation, which has been scattered by the instrument. It usually has the same aperture as the divergence slit.

6.2.3.4 Secondary Soller Slits

Systems that have a parallel primary beam usually have a specially adapted, secondary, Soller slit between the sample and the detector. Soller slits consist of closely spaced thin plates, made of a metal which absorb X-rays. Almost all diffractometers have Soller slits, to give better peak shapes. However, those fitted to parallel beam instruments are longer and the metal plates are parallel to ensure that the beam entering the detector is also parallel. The location of the secondary Soller slit is shown in Figures 6.12 and 6.13.

6.2.4 Detectors

There are several different types of detector which are fitted to residual stress diffractometers.

6.2.4.1 Proportional Detectors

These are “point” detectors; their design is described in Ref. 4. This type of detector has to be “scanned” across the peak and the diffraction pattern is collected sequentially. Consequently, when used for residual stress analysis, where good counting statistics are a necessity, they are rather slow. Proportional detectors have the advantage of being very robust. They are suitable for detecting the longer wavelength X-rays, from copper, cobalt, iron, manganese and chromium anode X-ray tubes.

6.2.4.2 Scintillation Detectors

Scintillation detectors are also point detectors; they have to be scanned across the peak. Their design is described in Ref. 4. They are more suited to shorter wavelength X-rays from copper anode tubes and are not very efficient for the longer wavelengths, for example chromium.

6.2.4.3 Position Sensitive Detectors (PSDs)

PSDs are "line" detectors. They consist of a wire or fluorescent screen that enables an angular "window" of data (usually about 15° 2-theta) to be collected simultaneously. They are particularly good for residual stress analysis where good quality data is required, quickly, over a relatively short angle range.

6.2.4.4 Area Detectors

Using an area detector a large section of the diffraction cone can be collected simultaneously. An example is shown in Figure 6.16. Area detectors are bulky, rather fragile and easily saturated by sample fluorescence, particularly as the K-β filter has to be placed in the primary optical path. However, it is possible to see any variations in intensity around the diffraction cone, which gives valuable information about grain size and texture (see examples in Figure 6.17).

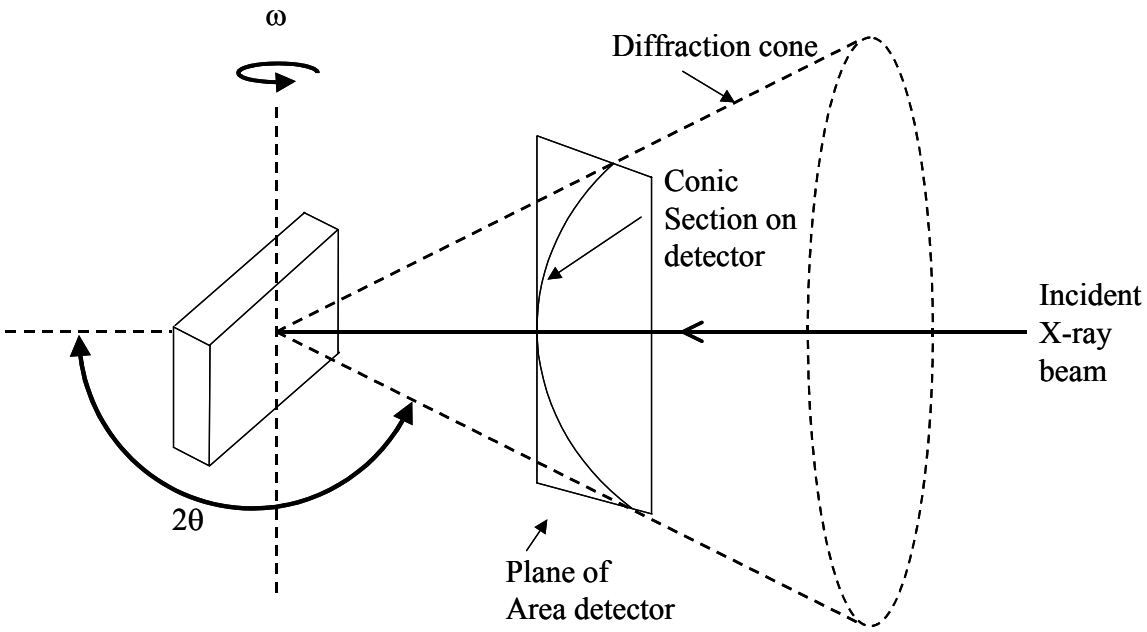

Figure 6.16 Conic section where the cone of the diffracted X-rays intersects the flat area detector

6.2.5 Secondary Monochromators

Point detectors (proportional and scintillation) can be fitted with secondary monochromators. The monochromator (a graphite crystal) transmits only the K-α radiation; the K-β, sample fluorescence and white radiation are blocked. Monochromators can be fitted to systems with either parallel or focused optics.

Obviously, not all of these components are compatible. Table 6.1 gives suitable combinations for parallel beam and focused system.

Table 6.1 Suitable combinations for focusing and parallel beam systems

	Primary Optics	**Secondary Optics**
Focusing systems	Divergence slit & beam mask	Receiving & scatter slits
Parallel Beam Systems	Poly-capillary or mirror	Secondary soller slits

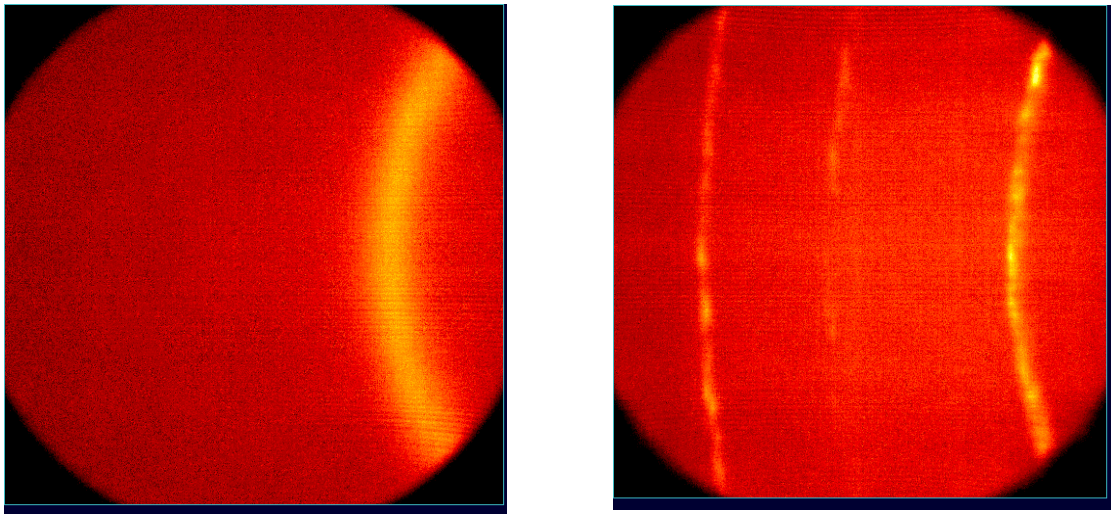

(I) (II)

Figure 6.17 Debye diffraction rings collected using an area detector

(I) Diffraction pattern from a sample of ferrite: here the grains are small & the intensity is even around the ring.

(II) Diffraction pattern from a sample of aluminium; here the grain size is larger, as can easily be observed from the uneven intensity distribution around the Debye ring. It is possible to integrate the intensity around a small section of the ring to reduce (but not eliminate) these intensity variations.

6.3 Portable Systems

These are much simpler than the lab-based systems. A portable diffractometer is shown schematically in Figure 6.18. The X-ray path length is much shorter than in a laboratory based system.

Figure 6.18 shows a schematic representation of a typical portable stress system. The instrument shown is an omega diffractometer. Combined chi and omega diffractometers are also available. The sample remains stationary, only the assembly carrying the tube and

detectors moves, allowing the machine to accommodate very bulky samples, or even to be placed onto a large structure.

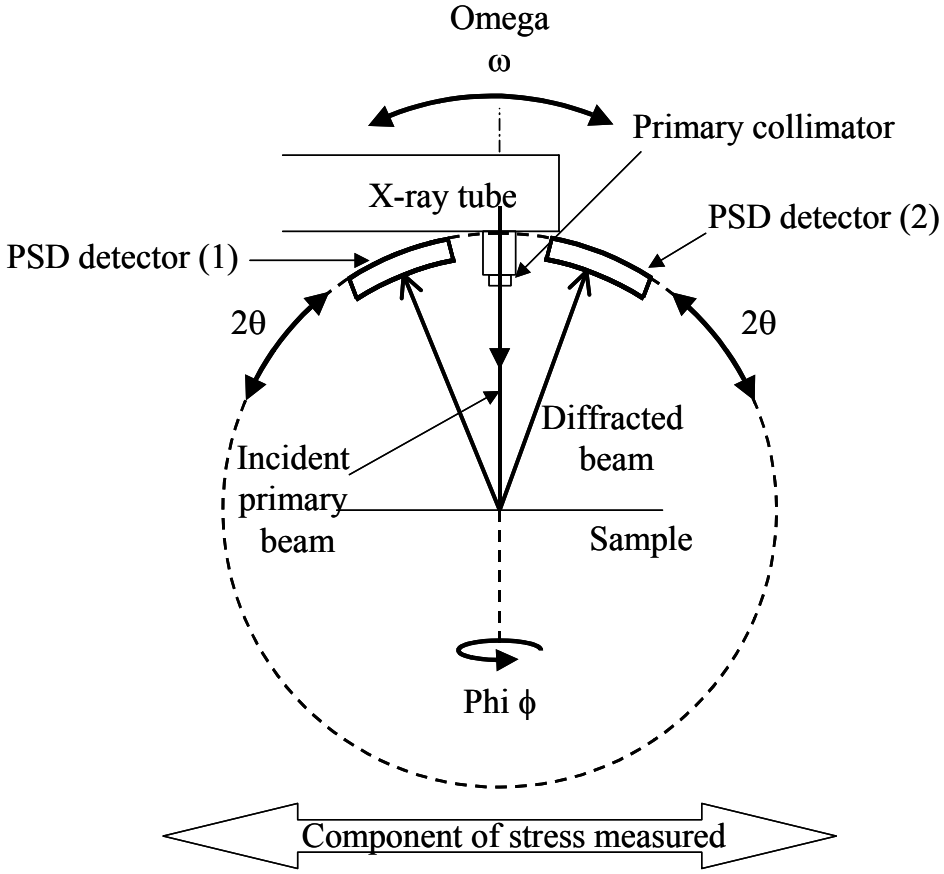

Figure 6.18 Typical portable stress measuring system shown in omega configuration

6.3.1 Primary Optics

6.3.1.1 Collimators

Portable stress diffractometers usually have a set of interchangeable collimators, either round or rectangular that limit the irradiated area.

6.3.2 Secondary Optics

Usually, there are just two small PSD type detectors, with a slot on each detector for installing a beta filter. Most portable systems have two detectors, which intercept opposite sides of the diffraction cone, enabling two psi offsets to be measured simultaneously.

6.4 Sample Positioning

It is important that the sample is placed exactly on the axis of rotation or the irradiated area will vary with psi. All instruments have devices to enable this.

> **Portable systems** have a small pointer attached to the goniometer head which touches the sample and then retracts a known distance.

Laboratory based systems usually incorporate a dial gauge.

7 Radiation Selection

The choice of X-ray tube anode and therefore the wavelength of the incident X-rays is critical for the measurement of residual stress.

The following criteria must be considered:

- **Sample fluorescence**
- **Diffraction angle**
- **Choice of crystallographic plane**

7.1 Sample Fluorescence

If the K-α_1 component of the incident beam causes the sample to emit its own fluorescent X-rays, the radiation is not suitable, even if the instrument is fitted with a secondary monochromator. An example is using copper K-α radiation with an iron sample. The copper K-α radiation has a slightly higher energy that the iron K-α absorption edge. The copper K-α radiation is exactly the right energy to be absorbed by the iron atoms and is then emitted as iron K-α, fluorescent radiation.

Fluorescence produces a very high background and consequently poor peak-to-background ratio. This can be dramatically improved by using a secondary monochromator, which will remove the fluorescent radiation before it enters the X-ray detector. However, as most of the incident X-ray beam is being absorbed by fluorescence, the penetration depth into the sample surface is very small and is insufficient for a representative stress measurement of a bulk sample.

Usually, a longer wavelength is selected, as this radiation will not have sufficient energy to cause fluorescence. For an iron sample a good choice would be a chromium anode X-ray tube. The longer wavelength (less energetic) chromium K-α radiation actually penetrates further in to an iron sample than the more energetic copper K-α.

7.2 Diffraction Angle, 2-Theta

The changes in the *d*-spacings due to the strain in the sample are very small, typically in the third decimal place. We need to select an X-ray wavelength that will give a reflection, from our sample, at the highest possible 2-theta angle.

According to Bragg's Law the *d*-spacing from which a diffraction peak is obtained using a particular incident wavelength is a function of sin θ, and obviously, the relationship is not linear. The change in position of a diffraction peak $\Delta\theta$ (and hence $\Delta 2\theta = 2\Delta\theta$) when there is a change in *d*-spacing, Δd, is obtained by differentiating Bragg's Law, which gives

$$\frac{\Delta d}{d} = -\Delta\theta \cot\theta \qquad \textbf{14}$$

At high 2-theta angles small changes in the *d*-spacing (like those due to strain) will give measurable changes in 2-theta, although the peak shifts are still only a few increments of a degree. At low angles the difference will be too small to be measured with any degree of precision.

Ideally, the radiation source should be selected to give a reflection at a Bragg angle greater than 130° 2θ. However, though not ideal, it is possible to use reflections which are as low as 125° 2θ. **Using reflections with 2-theta angles of less that 125° is not recommended**.

A wavelength should also be chosen that does not give a reflection too close to the high 2-theta limit of the instrument. Care must be taken to record the whole diffraction peak down to the background at both the upper and lower angular ranges.

7.3 Choice of Crystallographic Plane

Different crystallographic planes vary in their deformation mechanisms and give different responses for both elastic (residual stress) and inelastic strain (line broadening). Measurements made on different crystallographic planes are generally not comparable. Also, measurements made with different radiations may not be comparable due to the differing penetration depth of the X-ray beam into the sample, this is more an issue where steep stress gradients are present: see Section 5.4 for more details on penetration depths.

If it is suspected that the sample is textured, select the reflection with the highest multiplicity as this may reduce oscillation in the $\sin^2 \psi$ plot. If the sample has a large grain size it may also help to select the reflection with the highest multiplicity.

For accurate comparisons with previous data/measurements it is useful to check which planes have been used, historically, and if possible select the same ones.

Note: It is necessary to check the diffractometer alignment by measuring both a stressed and unstressed standard every time that the X-ray tube is changed or replaced.

Table 7.1 shows recommended X-ray tube and {hkl} plane combinations for a variety of materials.

Table 7.1 Recommended X-ray tube and {hkl} plane for some common materials

Material	Bravais Lattice	X-ray Tube anode	K-β Filter	Wavelength Å (All K-α1)	2-Theta Angle (Approx.)	{hkl}	Multiplicity[7]
Ferrite, α-iron	BCC[5]	Cr K-α	V	2.2897	156.1	{211}	24
Austenite, γ-iron	FCC[5]	Mn K-α Cr K-α	Cr V	2.1031 2.2897	152.3 128.8	{311} {220}	24 12
Aluminium	FCC[5]	Cr K-α Cr K-α Cu K-α Cu K-α	V V Ni Ni	2.2897 2.2897 1.5406 1.5406	139.3 156.7 162.6 137.5	{311} {222} {333}/{511} {422}	24 8 32 24
Nickel Alloy	FCC[6]	Mn K-α Fe K-α	Cr Mn	2.1031 1.9360	152 - 162 127 - 131	{311} {311}	24 24
Titanium Alloy	Hexagonal[5]	Cu K-α	Ni	1.5406	139.4	{213}	24
Copper	FCC[5]	Cu K-α * Cu K-α	Ni Ni	1.5406 1.5406	144.8 136.6	{420} {331}	24 24
Tungsten Alloy	BCC[6]	Co K-α	Fe	1.7889	156.5	{222}	8
Mo Alloy	BCC[6]	Fe K-α	Mn	1.9360	153.2	{310}	24
α Al_2O_3	Hexagonal[7]	Cu K-α Ti K-α	Ni Sc	1.5406 2.7484	152.8 156.5	{330} {214}	6 24
γ Al_2O_3	FCC[7]	Cu K-α	Ni	1.5406	146.1	{844}	24
TiN (Osbornite)	FCC[7]	Cu K-α	Ni	1.5406	125.7	{422}	24

* Be aware of K-β line fluorescence
Note superscripts refer to the source of the values as presented in the References.

8 Specimen Issues

8.1 Initial Sample Preparation

Prior to any residual stress measurement, any soil or grease should be removed, preferably by washing or by the use of a degreasing agent. **Mechanical methods such as grinding, machining or the use of a wire brush should be avoided, as they will introduce additional surface residual stresses into the sample being measured.** This is particularly important as the penetration of X-rays in most materials is in the range 5-50μm. If possible, samples should be measured in the as-received condition. Painted materials should be measured in the as-received condition in the first instance, as the presence of the paint layer will only result in a loss of intensity. However, paint layers can be removed chemically if necessary. If residual stress measurements are required on the surface of samples which show evidence of abuse, then light grinding or electropolishing may be necessary to produce a better surface, at the risk of altering the residual stress state of the sample.

The main requirement of a material for X-ray residual stress measurement is that it should be crystalline or semi-crystalline (there are reports in the literature of residual stress measurements on semi-crystalline polymers) and that it should have an isolated high angle diffraction peak, typically in the range 125-170° 2θ. Any sample selected for residual stress measurement should be representative of the material under investigation. The selection of the most suitable peak/radiation is dealt with in Section 7.

If cutting up of the sample is necessary then this should be carried out with care to avoid changing the existing residual stresses. Electro Discharge Machining (EDM) is a useful method for sectioning material without introducing significant residual stress, but care should be taken to avoid heating the sample as this could lead to relaxation of residual stresses. If the sample is large enough, then the residual stress measurements should be made as far as possible away from the free edge. If necessary, methods such as strain gauging should be considered to monitor any changes during or after sample cutting. It is therefore recommended that sectioning of samples should be avoided if possible.

8.2 Sample Composition/Homogeneity

The lattice spacing, which is used to measure the strain in a material, can also change as a result of compositional variation within the specimen, (e.g. within a carburised surface layer). The bulk composition of the material should therefore be constant within the irradiated volume. Because the penetration depth of the X-rays varies with ψ tilt, this must be taken into account when dealing with possible compositional changes.

It must be remembered that if the material is multi-phase, then the measured residual stress will be determined from the diffraction peak deriving from a particular phase only and the overall sample residual stress will be related to the stresses in each component phase and their volume fractions. It is therefore important that the peaks from each phase are clearly identified prior to residual stress measurement.

8.3 Grain Size

The grain size in the irradiated volume will have an important effect. In many crystalline materials grain sizes are in the range 10-100μm and these will be fine for X-ray stress measurement. Larger grain sizes will cause problems due to the fact that within the irradiated volume, only a few grains will be contributing to the diffraction peak, i.e. obeying Bragg's Law. A large grain size will mean fewer grains contributing and therefore lower peak intensities and less accurate peak location. In addition, the presence of micro/intergranular strains may affect results in large grained materials.

The related effect of texture also causes problems with residual stress measurement as it results in peaks of widely differing intensity with ψ tilt. This can be overcome to a certain extent by choosing appropriate tilts and also by oscillation (typically ±2 degrees) of the sample in ψ to bring more grains into the diffracting condition. If possible a pole figure of the lattice planes used for residual stress measurement should be obtained by a combination of measurement and/or calculation to help determine the most appropriate tilts to use.

8.4 Sample Size/Shape

For any sample, a suitable flat region should be chosen for residual stress measurement. This region should, if possible, be 1-2mm from the edge of the sample to avoid the effect of residual stress relaxation. The surface of the sample should coincide with the centre of rotation of the goniometer.

For residual stress measurement, the shape and size of the sample is not critical, although for laboratory systems, it must be able to fit onto the sample stage such that the various tilts can be performed. For portable systems, there is no upper limit in theory to the size of samples that can be examined, e.g. large diameter pipes, aircraft wings etc. as the machine is taken to the sample.

Sample weight is an important consideration for laboratory systems, because the sample will be subjected to various tilts during the measurement and therefore needs to be firmly attached to the specimen stage. Careful consideration as to how the sample is to be mounted and held onto the goniometer is required. The sample can be clamped to the stage only if this does not lead to additional residual stresses being induced into the specimen. Two examples are shown in Figures 8.1 and 8.2. Small specimens can be mounted on the stage using 'Plasticene', making sure that the surface to be measured is at the correct orientation. The relationship between the specimen and the incident X-ray beam/tilting direction will define the residual stress measurement direction.

One other important aspect is that it must be possible for both the incident and diffracted beams to interact with the specimen without being blocked. For example, if measurements are required at the root of a notch, then the method of tilting needs to be chosen such that there is a clear beam path from the X-ray tube to the detector.

Round samples can also be measured provided that the X-ray beam size is small in relation to the curvature of the specimen, i.e. the beam effectively 'sees' a flat area. For the hoop direction, measurement of residual stress within an accuracy of 10% requires a maximum spot size of R/4, where R is the radius of curvature of the sample. Intensities can be improved by elongating the beam in the axial direction. For axial measurements the maximum spot size should be R/2.

8.5 Surface Roughness

Given that no modification to the surface should be made, rough surface finishes can still be used for residual stress determination. However, careful interpretation of the results is needed, as the measured residual stresses will be more strongly influenced by the 'higher' regions of a rough surface. Recent work has indicted that the surface roughness caused by machining can affect the relationship between the lattice strains and evaluated stress via the X-ray elastic constants (XEC). This should be considered and XEC measurements performed if appropriate.

Recently, parallel beam systems (see section 6), have become available which do not require 'flat' samples.

8.6 Temperature

Generally, the temperature should be kept constant during a stress measurement to avoid additional changes in lattice parameter due to thermal expansion. A variation of a few °C is unlikely to affect the accuracy of any residual stress measurement.

If residual stress measurements are to be made at elevated temperatures, this will need to be carried out inside a furnace mounted onto the goniometer. Because of steep temperature gradients, the sample should be relatively small and care should be taken to ensure that the

temperature is constant not only over the time of the measurement but also over the specimen itself. The use of a vacuum or protective atmosphere may be required to reduce oxidation effects unless the residual stress in the oxide itself is being measured. Finally, some knowledge of the temperature variation of the elastic constants required to convert the measured strains into stresses will be needed.

8.7 Coated Samples

Coated samples can be measured fairly easily using X-ray diffraction, provided that diffraction peaks associated with the coating itself can be identified and isolated from any substrate peaks. If a steep stress gradient is present, then this will affect the results through curvature of the d vs. $\sin^2\psi$ plot. If this is the case then the use of a less penetrating radiation may help. Because of their processing route, it is also likely that coatings will be textured. Lastly, the values for the elastic constants for a coating may be considerably different from the 'bulk' values normally used. Readers are advised to consult the literature for further information on a particular coating system. There are a number of examples of residual stress measurements from coatings in the proceedings of the International Conferences on Residual Stresses.

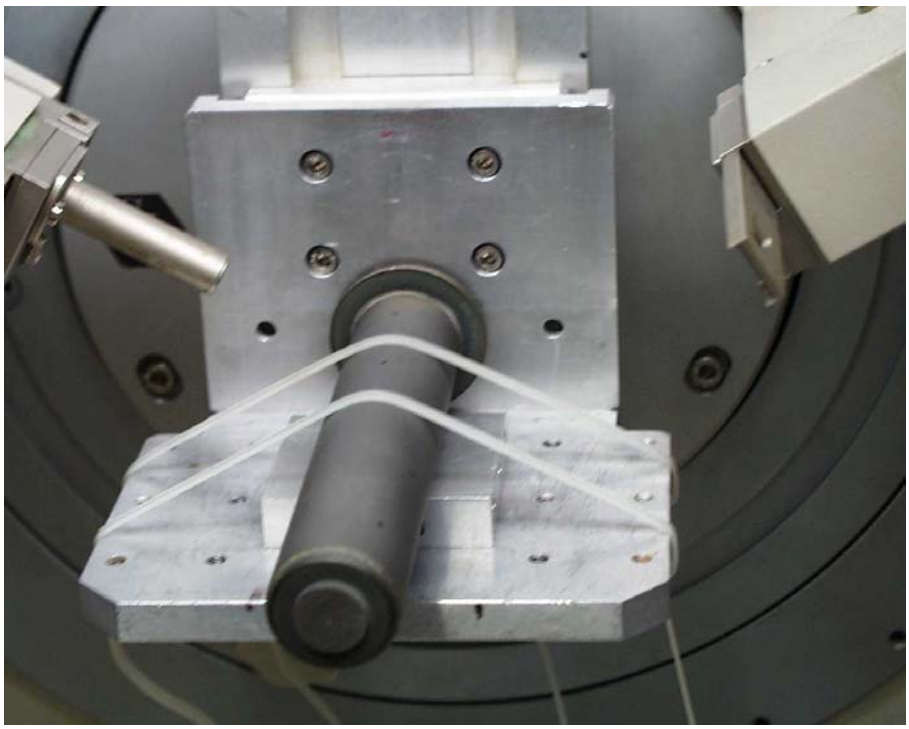

Figure 8.1 Photograph showing residual stress measurement in the hoop direction of a shot peened steel bar. Note the use of cable ties to hold the sample in place, along with a U or V shaped holder. (Courtesy of QinetiQ Ltd)

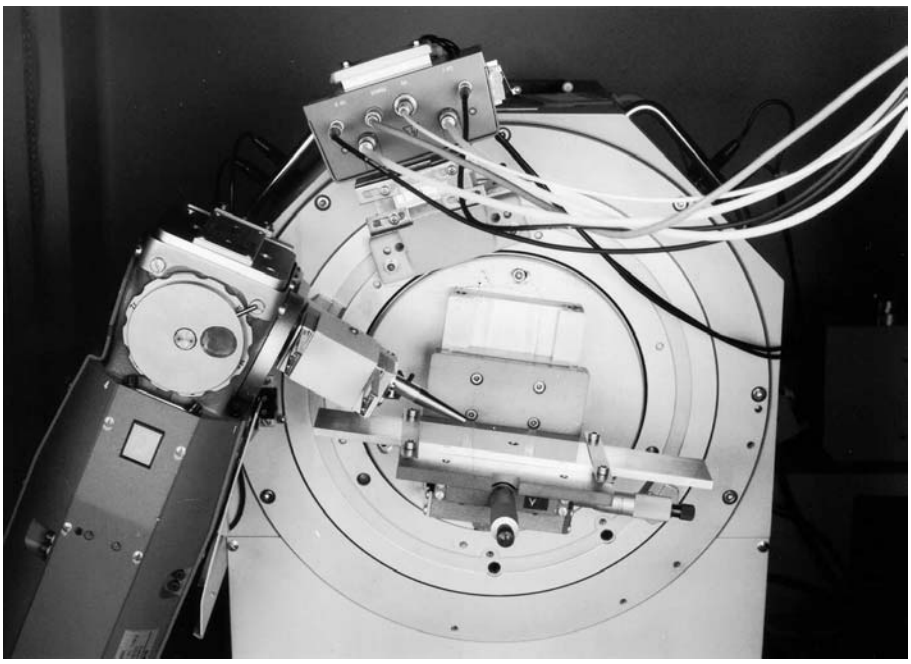

Figure 8.2 Photograph showing residual stress measurement close to a cold expanded hole in a high strength Aluminium alloy. The photograph shows the set-up for a negative Ψ tilt. Note the use of clamps to lightly hold the sample in place. It is also worth mentioning that the length of the sample can be quite long in the direction parallel to the X-ray beam, (140mm in the photograph), as the detector remains at a high 2θ position, (as shown), throughout the measurement. (Courtesy of QinetiQ Ltd)

9 XRD Depth Profiling Using Successive Material Removal

9.1 Material Removal Technique

The variation of residual stress can be determined as a function of depth by successive material removal by electro polishing and subsequent stress analyses. Any mechanical or electro discharge machining (EDM) technique used to remove surface layers will induce residual stresses, thereby altering the original stress field of the surface. Hence such methods should be avoided. **If layer removal is required chemical attack or electro polishing is the recommended method.**

9.1.1 Electro Polishing Theory

In the simplest case material removal can be achieved by submerging a metal sample into a tank containing a mixture of acids that are saturated with the metals salts. A voltage is applied across the sample and the tank (anode and cathode respectively) such that a current flows. After a period of time the voltage is removed and the sample washed. This process is commonly used for large scale electro polishing. On the laboratory scale material removal is usually more localized, and commercial equipment is readily available to perform such tasks. In this instance the sample is usually held over an aperture and the electrolyte is pumped onto the surface. A voltage is then applied for a set time, such that a certain amount of material is removed according to Faraday's first law. This states that the mass of metal removed Δm (i.e. the mass of metal ions) is proportional to the current ΔI^+ during time Δt, and is given by:

$$\Delta m = k \Delta I^+ \Delta t \qquad \textbf{15}$$

where k is the electrochemical equivalent of the sample material, which is equal to the mass of ions carrying 1 coulomb. On the basis of Faraday's second law the electrochemical equivalent for the reaction of $M \rightarrow M^{z+}+ze^-$ is given by:

$$k = \frac{A}{zF} \qquad \textbf{16}$$

where A is the atomic weight of the metal M, and F is Faraday's constant (96500 C).

The key to successful electro polishing is in the selection of electrolyte and polishing conditions. Electrolytes can be obtained from commercial sources or mixed in house, the selection of the correct electrolyte is beyond the scope of this document, and the reader is directed to the literature for further guidance.

Selection of the correct voltage conditions can be determined by performing a voltage scan on the material prior to polishing. By varying the applied voltage whilst the circuit is complete a graph such as that shown in Figure 9.1 can be obtained, which gives an indication of the correct voltage range to use for successful polishing.

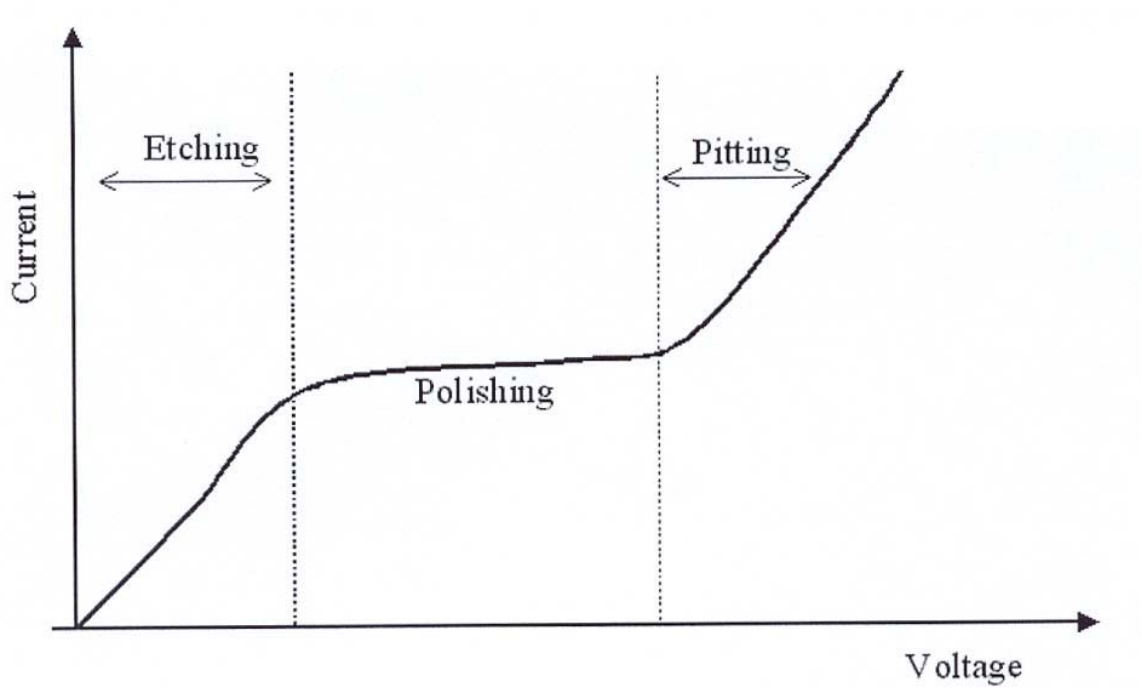

Figure 9.1 Idealised voltage-current scan for electro polishing.

Electro polishing can be performed on almost all metals, although there are several metals and alloys which do not lend themselves to standard practice, and will require some trials before an adequate surface finish is achieved. The suitability of a material to electro polishing is related to the process chemistry and the method by which the metal/alloy was processed. For example cast metals can be very porous making them difficult to electro polish.

9.1.2 Electro Polishing Problems

Although electro polishing is a reasonably straightforward process, problems can occur but with a little trial and error good surface finishes can be achieved. Table 9.1 shows some common issues that may occur along with the probable cause of this problem and a suggestion of how this issue can be resolved.

Table 9.1 Common problems that occur when performing electrolytic polishing and some suggested remedies commonly cited in the literature.

Problem	*Probable cause*	Suggestions
The centre of the polished region is too deeply attacked.	The polishing film did not form in the centre of the desired polished area.	• Increase the voltage of the electro-polisher. • Reduce the amount of agitation. • Use a higher viscosity electrolyte.
Pitting and attack at the edge of the specimen.	The polishing film is too viscous or it is too thin.	• Decrease the voltage of the electro-polisher. • Increase the amount of agitation. • Use a less viscous electrolyte.
Deposits are formed on the surface of the specimen.	The products formed at the anode are likely to be insoluble.	• Choose a different electrolyte which will not form insoluble products. • Raise the temperature of the system. • Increase the voltage of the electro-polisher.
The surface of the specimen is rough or has no lustre.	The polishing film is likely to be inadequate.	• Increase the voltage of the electro-polisher. • Try using a more viscous electrolyte.
There are undulations or scratches on the polished surface of the specimen.	Incorrect polishing time. Inadequate agitation. Unsuitable preparation.	• Try altering the amount of agitation. • Improve the preparation procedure. • Increase the voltage of the electro-polisher and decrease the polishing time.
There are stains on the polished surface.	Etching has occurred after the current has been switched off.	• Remove the specimen immediately after the current is switched off. • Choose a less active electrolyte.
Regions of the surface have not been polished.	There are likely to have been gas bubbles masking the surface.	• Increase the amount of agitation. • Decrease the voltage of the electro-polisher.
Different phases are in relief.	The polishing film is likely to have been inadequate.	• Increase the voltage of the electro-polisher. • Improve the preparation procedure used. • Reduce the polishing time.
Pitting.	Polishing time is too long. The voltage of the electro-polisher is too high.	• Improve the preparation procedure used. • Decrease the polishing time used. • Try various electrolytes.

9.2 Data Correction

When performing layer removal for residual stress depth profiling it is important to consider any redistribution or relaxation in the residual stress in the exposed surface, particularly if the component is relatively thin. Solutions are available to correct the stress values obtained.

9.2.1 Flat Plate

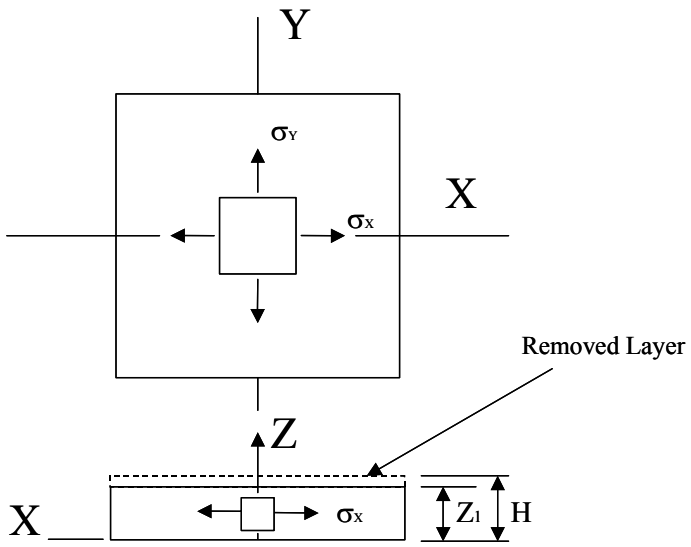

Figure 9.2 Stresses in a flat plate after layer removal

For a flat plate (Figure 9.2) a generalized solution proposed by Sikarskie (Ref 8) based on the original solutions of Moore and Evans (Ref 9) can be used. This takes the proposed solutions and expands the integrands in a Taylor's series, as shown below starting from the generalized solution:

$$\sigma(z_1) = \sigma_m(z_1) + 2\int_{z_1}^{H}\frac{\sigma_m(z)}{z}dz - 6z_1\int_{z_1}^{H}\frac{\sigma_m(z)}{z^2}dz \qquad \textbf{17}$$

Expanding the above integrands using a Taylor's series results in the following equation:

$$\sigma(z_1) = \sigma_m(z_1) + \left(\begin{array}{l} -4\sigma_m(H)\left(\frac{H-Z_1}{H}\right) + \left[\sigma_m(H) + 2H\sigma'_m(H)\right]\times\left(\frac{H-Z_1}{H}\right)^2 + \\ \frac{1}{3}\left[2\sigma_m(H) + H\sigma'_m(H) - 2H^2\sigma''_m(H)\right]\times\left(\frac{H-Z_1}{H}\right)^3 \cdots \end{array}\right) \qquad \textbf{18}$$

This can be simplified if electrolytic polishing is carried out over shallow depth increments (a few percent of the specimen thickness). In this case only the first term of the series is necessary for the correction of the raw data, thus:

$$\sigma(z_1) = \sigma_m(z_1) + \left(-4\sigma_m(H)\left(\frac{\Delta Z_1}{H}\right)\right) \qquad \textbf{19}$$

where H is the original plate thickness, ΔZ_1 is the change in thickness after layer removal, σ_m is the measured stress and σ_z is the corrected stress.

This correction has been shown to work well with flat plates, an example of this is shown in Figure 9.3, which shows results from XRD compared with Neutron diffraction for measurements on a shot peened plate of IN718 (Ref 10).

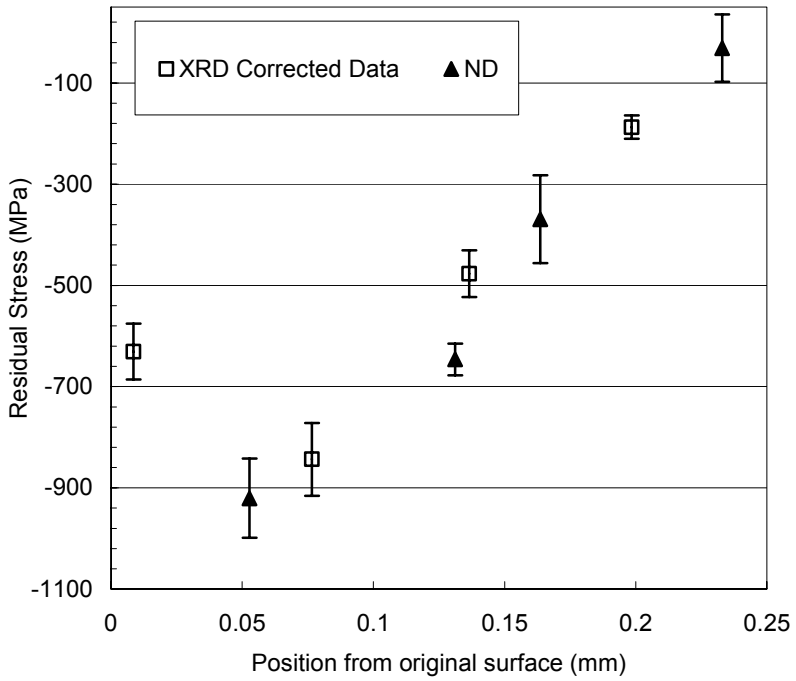

Figure 9.3 Comparison of XRD and ND (Pos A, B, C and D) near surface stress measurements on shot peened nickel based superalloy (IN718), using the flat plate correction.

9.2.2 Hollow Cylinder

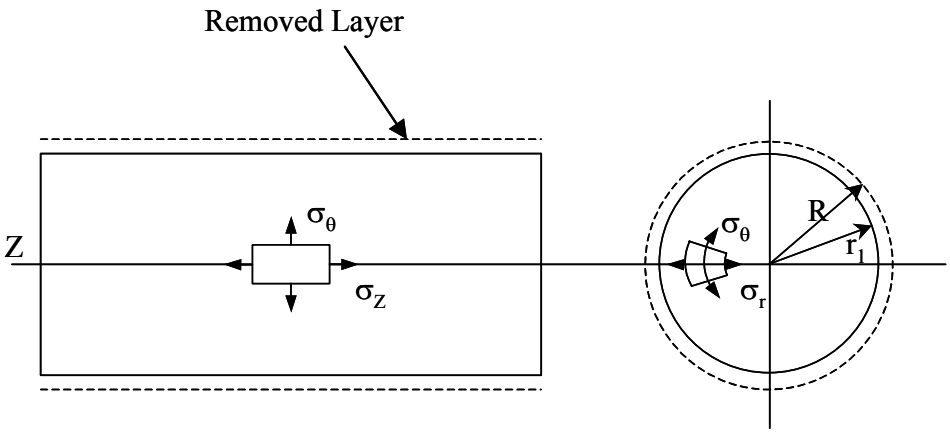

Figure 9.4 Rotationally symmetric stresses in a cylinder.

In the case of hollow cylindrical sample with rotational symmetric stresses, as shown in Figure 9.4, the following corrections can be applied.

$$\sigma_r(r_1) = -\left(1 - \frac{R_1^2}{r_1^2}\right)\int_{r1}^{R}\left(\frac{r^2}{r^2 - R_1^2}\right)\frac{\sigma_{\theta m}(r)}{r}dr \qquad \textbf{20}$$

$$\sigma_z(r_1) = \sigma_{zm}(r_1) - 2\int_{r_1}^{R}\left(\frac{r^2}{r^2 - R_1^2}\right)\frac{\sigma_{zm}(r)}{r}dr \qquad \textbf{21}$$

$$\sigma_\theta(r_1) = \sigma_{\theta m}(r_1) + \left(\frac{r_1^2 + R_1^2}{r_1^2 - R_1^2}\right)\sigma_r(r_1) \qquad \textbf{22}$$

where R is the original radius of the cylinder, and r_1 is the radius at the depth of interest.

Further examples of simple cases are presented in Ref 9.

9.3 Measurement and Data Presentation

9.3.1 Measurement of the New Surface Position

When making depth profiling measurements it is very important to be able to **accurately measure the amount of material removed**. This is achieved accurately measuring the position of the freshly exposed surface, and can be realised in several ways:

- Use a calibrated travelling microscope to focus on the newly exposed surface.
- Use of a calibrated dial gauge.
- Use of a calibrated micrometer.

In all cases it is recommended that a number of measurements be made over the freshly exposed service to ensure that the surface is flat. The mean value of these measurements is the recommended value to use in the data correction and final profile, as material removal can be uneven across a surface.

The depth increments used to measure the profile should be such that the profile is adequately measured and changes in gradient with depth recorded to the required level. In many instances the expected profile will be unknown and the operator should obtain guidance from the customer and perform measurements at the depth increments specified.

When presenting the data the operator should **avoid connecting data points as this infers that this is the exact stress profile**. This may not be the case and could unduly influence the customer and subsequent decisions. The **data points should include error bars to show the estimated uncertainty in position of the new surface**. The magnitude of these error bars will be dependant on the method used to locate the new surface, the degree of flatness, and the accuracy of the measurement. An example of depth profile data presentation is shown in Figure 9.5.

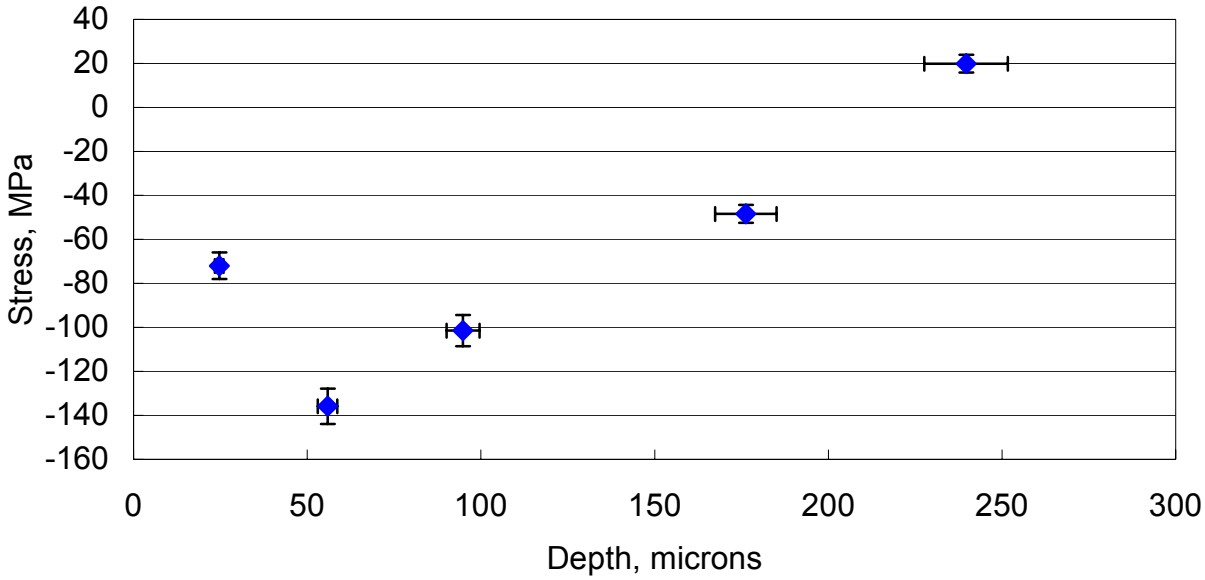

Figure 9.5 An example of data presentation for XRD residual stress depth profiling, showing errors bars for the stress uncertainty and the positional uncertainty, in this case an error of ±5% has been assumed.

Although time consuming this method has been shown to compare well to the Hole Drilling technique. XRD depth profiling whilst labour intensive does have the benefit of being able to perform repeat measurements prior to the next electro polishing step which is not the case with the Hole Drilling technique. Figure 9.6 shows a comparison of conventional Hole Drilling and Fine Increment Hole Drilling compared to X-ray diffraction on a machined

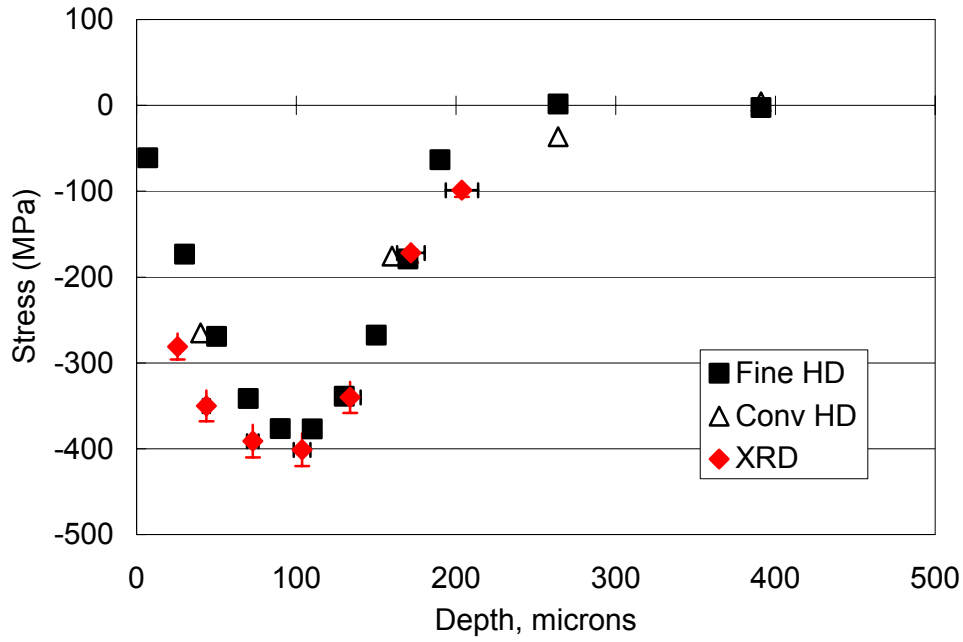

aluminium sample.

Figure 9.6 Comparison of residual stress profiles measured using XRD and fine and conventional increment hole drilling on a machined steel sample.

10 Measurement Procedure

10.1 Positioning of the Sample

The first step in performing a residual stress measurement is to position the sample on the diffractometer. The key requirement is to know where exactly on the sample the residual stress data is being obtained.

10.1.1 Goniometer Alignment

During a residual stress measurement, either the sample or the tube/detector fixture will undergo angular motion to select different ψ–angles (as covered in section 6, either a chi or an omega tilt maybe used in this selection, depending on the type of diffractometer and sample mounting setup which is available). The sample may also require translation to select different points on its surface, and/or rotation of the phi-angle to select different stress directions. It is important that all of these movements can be achieved without:

1 Changing the point at which the X-ray beam is incident on the sample.
2 Altering the height of the sample surface with respect to the incident X-ray beam.

The goniometer movements should be calibrated and verified by an optical method – e.g., using a theodolite or fixed viewer and a reference pin – to ensure that angular movements in phi do not cause the measurement position to change. The measurement position should lie at the centre of rotation of the phi and psi translators, and the rotation axes should intersect at the measurement position. This applies for both omega and chi tilting geometries.

A chi tilt can be verified by an optical method, or a simpler solution may be to measure on a standard sample – such as quartz or a sample with a known stress – to ensure that there is no unexpected movement of the diffraction peak when the sample is rotated to different psi–angles.

10.1.2 Sample Height and Beam Alignment

Ideally the sample should be positioned so that the surface lies precisely (within 100μm at worst) at the focus of the Bragg-Brentano circle. Height misalignment of the surface can introduce a shift in the position of the measured diffraction peak, and this must be considered if a highly curved surface is being studied. Nevertheless, accurate alignment of the diffractometer and specimen should be considered to be good practice in any measurement. The position of the sample surface should be invariant to any angular movement in phi or psi, and should also be unaffected by translation of the sample. If a sloping or otherwise non-planar surface is being measured at several locations, the sample height must be determined for each measurement location.

Adjustment of the goniometer alignment is generally undertaken by finding the position of the centre of rotation in phi and psi for the sample stage or cradle. These positions can be

recorded, or with most modern diffractometers, set to be 'zero' positions using the control software.

The incident X-ray beam should intersect the centre of rotation of the phi and psi translators. Verification that this has been achieved can be undertaken using a fluorescent screen, narrow aperture, or small standard sample. Displacement of the beam will introduce positional errors during rotation and/or translation of the specimen.

10.1.3 Calibration Using a Standard Sample

Alignment of the diffractometer can be verified by use of a standard stress-free sample. This could be, for example, a powder of known composition, a slice of mineral such as quartz, or a prepared sample with a known value of surface stress. Although many feel that stress-free standards are adequate for calibrations, recent results from a Round Robin exercise have highlighted the advantages of using a specimen with a well-characterised stress field for calibration verification purposes.

Such verification could form part of a regular check for the diffractometer, to highlight any need for full calibration to be performed.

The repeatability of a measurement on a standard sample can give an indication of the likely uncertainty in a stress measurement: see Appendix 1 for further information.

10.2 Measurement Directions

10.2.1 Theoretical Notes

Section 6 gives details of how the measurement direction is determined by the tilting of the sample during the measurement.

10.2.2 Principal Stress Directions

The stress tensor in a material can be written as:

$$\begin{bmatrix} \sigma_{xx} & \tau_{xy} & \tau_{xz} \\ \tau_{yx} & \sigma_{yy} & \tau_{yz} \\ \tau_{zx} & \tau_{zy} & \sigma_{zz} \end{bmatrix}$$

where σ denotes the normal stress components and τ the shear stress components acting at a point, using an *xyz* Cartesian co-ordinate system.

There exists a set of axes, called the *principal stress* axes, where the shear stress components are equal to zero. During stress measurement it is generally desirable to take measurements that are aligned with the principal stress directions. As one of the principal stress axes is almost always perpendicular to the sample surface, this means that it is generally not difficult to estimate the principal stress directions for X-ray measurement, simply by studying the geometry of the specimen.

If shear stresses are present, they will be manifested by splitting in the d *vs* $\sin^2\psi$ plot (see Section 5, Figure 5.5). If enough stress directions are recorded, it is possible to calculate the direction of the principal stress axes relative to the measurement axes. This is covered in the next section.

10.2.3 The Full Stress Tensor

A single set of psi values measured at a point will yield a value for the stress at that point, in the direction of the sample that is aligned with the scattering vector for $\psi = 90°$. If three sets of measurements are recorded, with positive and negative psi tilts, for three directions in the sample (usually two directions at 90° to each other, plus one at 45° in between), then the full stress tensor can be calculated, comprising the normal stress for each of the measured directions, and the shear stresses also. The values of the principal stresses, plus the angles between the principal stress directions and the measurement directions, can also be calculated. If only positive psi tilts are recorded, it may be difficult to determine if shear stresses are present.

For calculation of the stress tensor, it is generally assumed that the stress normal to the specimen surface, σ_{zz} or σ_3, is zero. There can be no stress normal to a free surface in equilibrium.

However, a stress can be maintained in this surface-normal direction at some depth below the surface. Hence for some deeply penetrating measurements (tens of microns), it is possible that a non-zero value of stress could be present. In this case, calculation of the stress tensor requires knowledge of the stress-free lattice parameter, d_0, for the material studied.

10.3 Measurement Parameters

10.3.1 X-ray Tube Power

Tube power is altered generally by changing the voltage and current applied to the tube. The X-ray tube should in general be operated at its maximum recommended power output, so that the diffraction peak can be recorded in the minimum time possible. **Specific tubes should always be operated at the same power setting, or different sets of measurements will be obtained from different depths below the sample surface. This impairs the reproducibility and comparability of measurements.**

10.3.2 Measurement Counting Time and Step Size

The counting time required to obtain a usable peak will vary depending on the tube and sample characteristics, the surface preparation method used, the presence of a K-β filter, and the presence of apertures in the incoming or diffracted beam paths to restrict the dimensions of the area from which information is obtained from the sample.

In general, the count should be long enough to ensure that a well-defined peak is obtained which does not show a poor outline because of statistical scatter. A useful method to determine an optimal count time is to record a peak at increasing count times until no further

improvement is obtained in the error when fitting the peak. **A rule-of-thumb is that 1000 counts should be more than adequate as a peak intensity.**

For materials, which, for various reasons, do not give well-formed, narrow or intense peaks, it is often worthwhile increasing the number of ψ-tilts recorded, rather than increasing the time to record each peak. Doubling the count time improves the counting statistics of each point in the peak by a factor of √2, whilst extra points on the *d vs.* $\sin^2\psi$ trace will improve the accuracy of the final stress calculation. It is important to consider that in X-ray stress measurement the accuracy of the individual peak is not the critical factor in determining the error in the final result.

The intensity of the diffraction peak is likely to be different for each psi-angle recorded, because of the different path length in the sample at each angle. Large changes in intensity are indicative of a highly textured material (see section 9.4).

Selection of count times does depend to a certain extent on the type of detector being used, and the number of points (or step size) selected for the diffraction peak. This is covered in the following sections.

10.3.2.1 Position-sensitive detectors (PSDs)

As a PSD records the diffraction intensity simultaneously over an angular range of several degrees, a total count time only is generally required. Depending on the type of PSD, data is generally 'binned' into a specified number of angular channels. The wider the angular range in each bin, the quicker the recorded intensity will accumulate in each. However, a wider bin gives a lower resolution in peak position. **Typically, a bin size of 0.05° is adequate. At least 20 data points are generally required over the entire peak for good peak location.**

For particularly broad peaks, or when recording a spectrum with two adjacent peaks, it may be necessary to scan the PSD in 2-theta. Whether this is possible will depend on the software used for data acquisition. Again, a suitable counting time must be selected to ensure adequate peak intensity.

10.3.2.2 Single detector

With a single detector system, instantaneous measurement can be obtained at a single value of 2-theta only. The detector must be scanned through a range of 2-theta to build up a profile of the X-ray intensity comprising the diffraction peak. The range of 2-theta will depend on the width of the peak being studied, but for most materials is unlikely to be smaller than 3°; a sufficiently wide range must be chosen to capture the entire peak at all psi-tilts. As with the PSD, a step size must be selected, and this will typically be in the range 0.05° to 0.2°. A smaller step size will give a more accurate final peak fit, but will of course increase the amount of time to acquire the peak.

10.3.3 Number of Tilt Angles Required for Stress Determination

In order to provide an indication and quantification of shear stress present in a sample, **it is recommended that at least 5 tilt angles are used for both positive and negative psi.** If the material is highly textured (see section 9.4) or a poorly-defined diffraction peak is obtained, recording extra psi-tilts may improve the accuracy of the final stress calculation. In general, $\sin^2\psi$ values between 0 and 0.5-0.6 are recorded. However, in cases where the sample

geometry does not permit tilting, or where there is strong texture, $\sin^2\psi$ values as low as 0.12 may be used, as long as it is appreciated that this will give a lower accuracy result, particularly if there is significant shear stress present.

Portable diffractometers allow for simultaneous collection of two psi-angles simultaneously through the use of two detectors.

Depending on the type of cradle used to mount the sample, positive and negative ψ movements may not be possible. If one psi movement only is possible, the opposite sign of psi-value (termed the 'pseudo-negative' psi) can be obtained by rotating the sample by 180° in phi (in the plane of the surface).

10.4 Dealing with Non-Standard Samples

10.4.1 Large-Grained Samples

If a sample has a large grain size in the region being sampled (approaching the order of mm in size), then counting statistics – and scatter in results owing to a low sample of number of grains – will be poor. There may be very few grains contributing to the diffraction peak. The only solution to this problem is to try to increase the number of grains that are contributing to the diffraction peak. Generally the options are:

- translate the sample during the measurement in order to cover a larger area of the surface;
- oscillate the sample in the phi-rotation, to increase the number of grains meeting the criterion for diffraction;
- oscillate the sample in the psi rotation, again in order to increase the number of grains meeting the criterion for diffraction.

Translation of the sample is not an option if the stress is not uniform over a reasonable distance (say several millimetres), and of course is not recommended if a stress profile across the surface is being constructed. **Translation of ±2mm during a measurement in both x- and y-axes can often give a marked improvement in the diffraction peak profile.**

Oscillation in phi is relatively benign, and oscillations of up to 5° can be made without significantly impairing the accuracy of the stress in terms of the measurement direction.

Oscillation in psi can also be beneficial, but will mean that a single point on the *d vs.* $\sin^2\psi$ plot will have an uncertainty in psi.

For any oscillation, there should be at least one full oscillation cycle during the measurement period.

10.4.2 Highly-Textured Materials

Textured materials can also benefit from the use of oscillations as described in section 9.4.1. However, for particularly strong textures, the only solution may be to switch to using a different diffraction peak.

10.4.3 Multiphase Materials

In multiphase materials, such as composites or alloys where there is a large volume of a second phase, it may be necessary to record the stress in both phases of the material, or at least to be aware that the stress recorded in a single phase may not be a complete description of the stress state in the material.

If the second phase is present in a small fraction (say less than 10% by volume), then counting times may be prohibitively long.

Care needs to be taken to ensure that diffraction peaks from the two phases are not overlapping or coincident. Some analysis software may not be able to cope with attempting to fit more than one peak at a time.

10.4.4 Coated Samples

Measurement of the stress in a coating should not be problematic provided that the coating is reasonably thick (typically several hundred nm), fine-grained and crystalline. Depending on the coating/substrate combination, it may be possible to select a radiation wavelength which allows measurements to be obtained in both coating and substrate, but see the notes on multiphase materials in the preceding section.

Coatings which have extremely fine crystalline regions (on the nm scale) may benefit from grazing-incidence methods, but these are outside the scope of this Guide.

10.4.5 Materials with Large Stress Gradients

A particularly high stress gradient (over 10 MPa/μm, but may be more or less depending on the penetration of the X-rays) will cause curvature in the d *vs* $\sin^2\psi$ plot, as a different mean penetration depth is obtained at each tilt angle, giving a different stress. Different results can be obtained with different wavelengths, owing to the different penetrability's.

A possible solution is to use a low-energy wavelength with limited penetration into the material.

10.5 Data Analysis and Calculation of Stresses

Analysis of the diffraction peaks, and calculation of the stress, is likely to be performed using proprietary software supplied with the particular diffractometer being used. Data required by the user include the Young's modulus and Poisson ratio for the material studied, and either

the crystalline anisotropy factor for the material or the diffraction elastic constants for the lattice planes used in the measurement.

Care should be exercised when choosing the X-ray elastic constants (XEC) to use in the stress analysis. If the final residual stress value is to be used for purposes other than batch comparison it is recommended that separate measurement of the XEC's be performed by the user on the material of interest. Potential errors possibly in excess of 20% are possible if incorrect values are used. Errors of this magnitude could be catastrophic if the data is to be used for structural or lifing assessments where precise values are required. If the measurement is to be used as a form of quality control, or batch comparison etc, then knowing the precise value is not as important as being able to monitor if the value changes, and so this issue is of less importance.

It should also be noted that within the literature there is scatter between the XEC values quoted for particular materials, depending on the model used, or direct measurement method used. It is important to be aware of this when setting the variables for the residual stress analysis.

Further description of the data analysis options is given in Appendix 2.

A critical part of data analysis for X-ray stress measurement is to make an early assessment of the quality of the diffraction peaks over the entire range of tilt angles.

10.6 Errors and Uncertainty

As noted previously, the error in the final stress value is dependent primarily on the fit to the *d vs.* $\sin^2\psi$ plot. Errors in the determination of the individual peak positions will degrade the accuracy of the final result. More points on the *d vs.* $\sin^2\psi$ plot – *i.e.*, more tilt angles – should give a more accurate result, provided that the peaks can be fitted accurately by the software used and that there are no unusual features such as texture present.

The total uncertainty in a measurement will contain other factors in addition to the error in the diffraction peak position. Uncertainty in the bulk Young's modulus, or the plane-specific modulus, will introduce error into the final result, although such errors are systematic – in that they will have the same effect on all measurements – rather than random in nature, as are the counting statistics associated with peak recording. A fuller discussion of issues relating to uncertainty in the final value is given in Appendix 1.

It is important to realise that the ± "uncertainty" values produced currently by commercial measurement software only reflect the estimated statistical errors in (or goodness of fit of) the $\sin^2\psi$ plot.

11 Reporting of Results

Detailed reporting of results is not restricted to the provision of data to an external customer. Basic record keeping of individual measurements allows for future traceability of data and re-interpretation of results.

For any particular measurement, it is recommended that the parameters described in the following section be recorded for each measurement as a minimum requirement. An example of a measurement proforma is included at the end of this section.

11.1 Value of Residual Stress

The stress value determined by the measurement, along with its error as stated by the software fitting routine that was applied.

11.1.1 Uncertainty

If the uncertainty in the measurement has been calculated, by a combination of errors from repeated measurements and uncertainties in quantities such as the Young's modulus (see Appendix 1 for more information on such methods), it should be reported. Hence the uncertainty in the measurement may be greater than the error as quoted by the fitting routine.

11.1.2 Stress Direction

The direction in which the stress was measured should be noted. This is recommended even in the case where an isotropic stress field is anticipated. In the case where the principal stress axes are unknown, the stress direction may be given in reference to an identifiable geometric axis of the specimen.

11.1.3 Depth Position

If a profile of the stress with respect to depth has been performed, it is recommended that the depth position at which the measurement was made should also include an estimate of the uncertainty in this position.

11.2 Diffraction Set-up

11.2.1 X-ray Wavelength

The tube characteristics should be recorded:

- emission source used;
- X-ray K-α wavelength produced;
- tube voltage and current used.

11.2.2 Diffraction Peak

The lattice planes used for the experiment should be recorded, along with the angle 2-theta of the diffraction peak.

It is recommended that a record is kept of the full width at half maximum height (FWHM) of the peak. The peak intensity may be useful to record for comparison purposes if the counting time is noted also.

It is sensible to keep a record of a typical raw diffraction peak from the measurement set for reference purposes. If the peaks recorded are atypical (because of texture, for example), it may be appropriate to report all peaks along with the results.

11.2.3 K-β Filtering

If a filter is used to remove the contribution of the K-β emission from the X-ray source, this should be indicated, along with the material comprising the filter.

11.2.4 Optical Set-up

Details of any apertures, collimators *etc*., which are placed in the incident or diffracted beam path, should be recorded. This should include their position and the dimension(s) of the aperture. If appropriate, the dimensions of the irradiated area on the sample, when the surface is normal to the incident beam, should be stated.

11.3 Position of the Measurement

The position on the sample from which the measurement stated in 10.1 was obtained, with an indication of the origin point on the sample from which the measurement position can be located.

The likely uncertainty in the position should be reported.

(In the case where the surface stress is expected to be isotropic over a large area, the measurement position is unimportant and may be omitted, provided that a position has been selected which is unlikely to be influenced by sample edge effects.)

If a depth profile of stress is being generated, the depth of each measurement should be recorded relative to the initial surface position. If depth variation is obtained by changing the incident X-ray wavelength or intensity, the position of the diffracting gauge volume centroid below the surface should be reported, along with an indication of how its position has been calculated.

11.4 Additional Recording Parameters

These parameters are particularly recommended for reporting where the data are being passed to an external customer.

11.4.1 Fitting Routine

Details of the fitting routine used, or, if not known, the name and version of the software package used to analyse the data.

Any variable parameters used in the peak fitting routine: *e.g.*, constant or sloping background selected, percentage of the peak used for a centre of gravity calculation, *etc*.

11.4.2 Material Properties

The mechanical property values used for stress calculation should be noted, even if supplied by the fitting software. These values are generally at least the bulk Young's modulus, Poisson ratio, and crystal anisotropy factor for the material. Alternatively, the stiffness of the lattice planes measured (the diffraction elastic constant or DEC) can be noted if this is known or assumed.

11.4.3 Surface Preparation Method

Details of any treatment applied to the sample prior to stress measurement which will have altered the condition of the surface. Examples are grinding, polishing (mechanical or electrochemical) and chemical treatments.

If a depth profile of stress is being measured using material layer removal, details of the method by which material is removed should be noted.

11.4.4 Machine Characteristics

Details of the spectrometer used to perform the measurement: manufacturer, model number, detector type *etc*.

11.4.5 Sample Details

General details about the sample, including, as appropriate:

- composition;
- thermal and/or mechanical history;
- grain size;
- texture.

11.4.6 Other

Any other information which is relevant to the specimen, diffraction set-up or data analysis. In particular, any factors which may have an adverse effect on the reliability of the quoted results.

The proforma on the following page is a good basis for identifying what needs to recorded and can be copied and adapted for recording the results and test setup for your organisation.

An Example of a Residual Stress Measurement Proforma

Operator: _____ **Test Date:_____**

Section 1 Sample Information

Sample reference no:	**Sample details**
Surface preparation method	

Section 2 Machine Information

Machine used	**Tube element**	**X-ray K-α wavelength**
Tube voltage	**Tube current**	**Detector used**
Apertures used	**Tilt geometry and tilt angles used**	
Counting time	**Diffraction peak used**	**Diffraction angle range**

Section 3 Stress result

This section may contain a single stress result, or a Table or graph of a series of results could be appended. Information on measurement positions, errors and uncertainties should be provided as appropriate.

Residual stress =_____ **Error = ±_____**

Uncertainty* = ±_____

The above reported expanded uncertainty is based on a standard uncertainty multiplied by a coverage factor k=2, which corresponds to a level of confidence of approximately 95 percent.

***** See Appendix 1 for definition

12 Summary

Every case will be different but it is useful to consider the following points when performing residual stress measurements using X-ray diffraction:

- **Care should be taken with the specimen preparation especially where the surface of the specimen requires modification or cleaning. Mechanical methods such as grinding, machining or the use of a wire brush should be avoided, as they will introduce additional surface residual stresses into the sample being measured.**

- **If it is likely that comparisons are to be made using the data then bear in mind that the experimental conditions should be nominally the same. For example specific tubes should always be operated at the same power setting, or different sets of measurements will be obtained from different depths below the sample surface. This can have a significant effect on the reproducibility and comparability of measurements.**

- **For accurate comparisons with previous data/measurements it is useful to check which planes have been used historically, and if possible select the same ones.**

- **It is recommended that high 2-theta peaks be used for the measurements. Using reflections with 2-theta angles of less that 125° is not recommended.**

- **A high count rate is needed to enable reliable peak fitting. Generally narrow receiving slits (less than 0.2 mm) are not suitable for residual stress analysis since the count rate is reduced and so the measurement time has to be increased.**

- **For most tests, a peak intensity of 1000 counts should be sufficient as a peak intensity.**

- **In addition to a high peak intensity, it is also desirable to have a well-defined peak. At least 20 data points are generally required over the entire peak for good peak location.**

- **To reduce errors in the stress evaluation it is recommended that at least 5 tilt angles be used for both positive and negative psi.**

- **In some cases, for example where large grains are evident or where the specimen is textured, oscillating the sample can improve the quality of the measurement. Translation of ±2mm during a measurement in both x- and y-axes can often give a marked improvement in the diffraction peak profile.**

- **Oscillations in phi are relatively benign, and oscillations of up to 5° can be made without significantly impairing the accuracy of the stress in terms of the measurement direction.**

- **Oscillation in psi can also be beneficial, but will mean that a single point on the *d vs.* $\sin^2\psi$ plot will have an uncertainty in psi.**

- **A critical part of data analysis for X-ray stress measurement is to make an early assessment of the quality of the diffraction peaks over the entire range of tilt angles. From this first assessment decisions on the peak treatment can be made.**

- **It is then recommended that the peak be corrected for asymmetry arising from the presence of the K-α_1 and K-α_2 doublet (See Appendix 2).**

- **In general diffraction peaks are closer to a Gaussian than a Lorentzian shape, which makes the Gaussian function a good choice for peak fitting for standard X-ray stress measurement applications (See Appendix 2).**

- **If the variation of residual stress with depth is required chemical attack or electro polishing is the recommended method. Electro polishing can be performed on almost all metals. It is important to accurately measure the amount of material removed, and include error bars to show the estimated uncertainty in the position of the new surface when presenting the data. Also it is recommended that connecting the data points be avoided, as this infers that this is the exact stress profile.**

In cases where inadequate diffraction peaks are obtained it maybe beneficial to consider the following list of possible problems with the measurement:

Large grain size

Not enough diffracting grains to give a smooth intensity distribution in the peak.

Texture

The peak can totally disappear or its shape can be distorted in some $\pm\psi$ positions.

Too low net intensity

The lower the intensity, the higher the scatter in the results of the peak shift determination. However, there is a limit in increasing the intensity beyond which no further benefit in reduced scatter is obtained.

Superposition of many diffraction peaks

This typically happens when there is more than one phase in the sample.

Distorted diffraction peaks

Caused, for example, by a steep stress gradient, or distortion of the crystal lattice (such as cubic distorted to a tetragonal structure typical for hardened steels with a high carbon content).

Truncated broad peaks, where the background is not well defined

This is a typical situation with many position-sensitive detectors, the width of which can be between 10 and 20°. In this case, applying a linear background

subtraction causes large errors because the background noise has been incorrectly described.

References

1 B.D. Cullity. Elements of X-ray diffraction, second edition, Addison Wesley.

2 I.C. Noyan and J.B. Cohen, "Residual Stress – Measurement by Diffraction and Interpretation", *Materials Research and Engineering*, Springer-Verlag, New York Inc., 1987.

3 *Residual Stress Measurement by X-Ray Diffraction – SAE J784a*, Society of Automotive Engineers Inc, N.Y., USA, 1971.

4 Introduction to X-Ray Powder Diffractometry, Ron Jenkins & Robert L Snyder, John Wiley & Sons, 1996.

5 Structural and Residual Stress Analysis by Non-destructive Methods, Evaluation, Application, Assessment. Viktor Hauk, Elsevier, 1997.

6 CEN TC 138, Non Destructive testing – Test Method for Residual Stress by X-Ray Diffraction. European Standard Working Document. PrEN 15305, July 2005 (currently in draft form only).

7 Ceramic Data Supplied by Stresstech, Tikkutehtaantie 1, FIN-40800, VAAJAKOSKI, Finland.

8 D.L. Sikarskie, "On a series form of correction to stresses measured using X-ray diffraction", AIME Transactions, Vol. 239, 1967, pp. 577-580.

9 M.G. Moore and W.P. Evans, "Mathematical correction for stress in removed layers in X-ray diffraction residual stress analysis", SAE Transactions, Vol. 66, 1958.

10 N.W. Bonner, R.C Wimpory, G.A. Webster, A.T. Fry and F.A. Kandil, "Measurement of residual stress through a shot peened surface subjected to successive material removal", Materials Science Forum Vols. 404-407, pp. 653-658.

11 BIPM, IEC, IFCC, ISO, IUPAC, OIML, "*Guide to the expression of uncertainty in measurement"*. International Organisation for Standardisation, Geneva, Switzerland, ISBN 92-67-10188-9, First Edition, 1993 (This *Guide* is often referred to as the GUM)

12 A.M. Jones, "Residual stresses: A review of their measurement and interpretation using X-ray diffraction", Report AERE-R13005, Harwell Laboratory, Didcot, Oxfordshire, England, May 1989.

13 F.A. Kandil et al. (Eds.), "Manual of Codes of Practice for the determination of uncertainties in mechanical tests on metallic materials", Project UNCERT, EU Contract SMT4- CT97-2165, Standards Measurement & Testing Programme, ISBN 0-946754-41-1, Issue 1, September 2000.

Appendix 1

Sources of Measurement Uncertainty

A1.1 Introduction

Uncertainty is the amount of doubt in the result of a measurement. It is usually described by a parameter that defines the range within which the true value of the quantity being measured is estimated to fall (within a given confidence – usually 95%). At all stages in the measurement and subsequent analysis of data there exist potential sources of error. It is essential to distinguish the term 'error' (in a measurement result) from the term 'uncertainty'. Error is the measurement result minus the true value of the quantity being measured. Whenever possible, a correction equal and opposite to the error should be applied to the result. To evaluate measurement uncertainty, all sources of uncertainty must, as far as practically possible, be identified and their respective contributions quantified. A route map for evaluating uncertainty and further background information is available in Ref. 11.

A1.2 Sources of Uncertainty in Residual Stress Measurement

During the measurement of residual stresses there are a number of factors that contribute to the uncertainty of the measurement, including the alignment of the diffractometer or portable measuring apparatus, which must be optimised, and the specimen under examination must be correctly positioned with respect to the apparatus. Also, the diffraction data is statistical in nature and must be corrected for various geometrical and specimen-related factors. The diffraction peak position must be established by some profile or curve fitting method which introduces some uncertainty in the results. The strain data obtained must be transformed into stresses using some form of elastic constants. There may also be problems of non-linearity due to texture, coarse grain size, stress gradients with depth and micro-stresses due to plastic deformation or grain interactions. Many of these are non-quantifiable although theoretical analyses and modelling are being developed to solve these problems. Some of the experimental and analytical methods of dealing with these non-linearities introduce their own error contributions [12].

It is important to realise that the ± "uncertainty" values produced currently by commercial measurement software only reflect the estimated statistical errors in (or goodness of fit of) the $\sin^2 \psi$ *plot. It should not, therefore, be confused with the measurement uncertainty as defined in the GUM* [8] *and in this Guide, which should reflect all sources.*

In summary, the main sources of uncertainty in this measurement are listed below:

- Elastic constants (E & ν)
- Instrument alignment
- Specimen-surface height offset
- 2θ step size
- Number of ψ tilts
- Length of counting time
- Peak-fitting analysis method
- Stress analysis algorithm and software
- Specimen material
- Non-linearity due to texture, coarse grain size, stress gradients with depth, etc
- Specimen surface condition (in terms of surface finish & flatness)
- Operator competence (including interpretation of results)

A useful source of information on many of the above-listed experimental errors associated with X-ray measurement of residual stress can be found in Chapter 6 in Ref. 2.

A1.3 Evaluation of Uncertainty in the Measurement

As the effects of many of the sources identified above are non-quantifiable, any method of evaluating the uncertainty must be verified via an inter-laboratory exercise that involves as many laboratories as possible that are deemed competent in the measurement and adhere to the procedures described in this Guide.

Detailed below is a very simplified method that can be used in a single laboratory. It assumes that all systematic errors have been either eliminated or corrected.

The repeatability of the measurement can be quantified in either of 2 ways:

(i) Set the equipment to perform a number of consecutive tests (e.g. 10) using identical conditions and without removing the specimen between measurements. In this case, the only variables are those relating to the performance of the measurement system and the associated statistical (random) effects in data capturing and analysis by the software. For simplicity, this will be referred to as "*instrument-only repeatability*".

(ii) As above, but with the specimen removed completely in between measurements. In this case, effects due to variability in the test set-up are introduced. These will include resetting the device and the precision of repositioning the sample. This will be repeated as the "*instrument-operator repeatability*"

It is good practice to repeat any measurement as many times as practically possible. However, it is not always possible to do this in every "routine" set of measurements. It is recommended therefore that the above repeat measurements are performed (i) as part of instrument accreditation or regular quality check for producing satisfactory results (carried out at specific intervals or whenever the tube is changed for example), and (ii) if the customer demands it.
Table A1.1 shows an example of results obtained at NPL in two series of repeat tests on a shot-peened spring-steel plate sample. Series 1 results were obtained from 10 repeat

measurements without removing the sample from the machine between successive tests. Series 2 results were obtained from the same specimen but in this case the specimen was removed from the machine between successive tests. As can be seen, the mean values in both series of tests are very similar and it is anticipated that as the number of tests increases, the two values will converge to a unique single value. This is due to the randomness of the parameters causing the variability. The standard deviation in Series 2, however, is almost twice that in Series 1. The difference reflects operator-related effects. The table also includes some relevant estimated quantities that were derived from the repeat tests.

Table A1.1 - Results of repeatability of residual stress measurements (MPa) in a shot-peened spring-steel plate sample (Analysis: Pseudo-Voigt method)

Series*	Test 1	Test 2	Test 3	Test 4	Test 5	Test 6	Test 7	Test 8	Test 9	Test 10
1	-536	-529	-529	-530	-539	-531	-533	-535	-533	-528
2	-533	-535	-529	-525	-538	-550	-543	-550	-543	-546

Series	Max, MPa	Min, MPa	Mean, MPa	STD, MPa	Error‡, MPa
1	-528	-539	-532	3.6	±26
2	-525	-550	-539	8.6	±27

* Series 1 = instrument-only repeatability
Series 2 = instrument-operator repeatability

‡ Average estimated values produced by the analysis software

A1.4 Symbols and Definitions for Uncertainty Evaluation

To evaluate the measurement uncertainty, the following symbols and definitions are used. For a complete list see Ref. 13:

Coverage factor, k
A number that, when multiplied by the combined standard uncertainty, produces the expanded uncertainty. It is dependent on the confidence level (e.g. 95% probability).

Standard uncertainty, u
The estimated standard deviation.

Combined standard uncertainty, u_c
The result of the combination of standard uncertainty components. It is computed using the root sum squares:

$$u_c(\sigma)=\sqrt{\sum_{i=1}^{m}\ [c_i u(x_i)]^2} \qquad \textbf{15}$$

Where $u(x_i)$ is the estimated uncertainty in input quantity x_i

Expanded uncertainty, U $(U=k\,u_c)$
The value obtained by multiplying the combined standard uncertainty by a coverage factor.

Residual stress, σ
The estimated mean stress value in MPa.

d_v
Divisor used to calculate the standard uncertainty

$= 1$ (for normal probability distribution)
$= 2$ (for normal probability distribution, $k = 2$)
$= \sqrt{3}$ (for rectangular probability distribution)
$= \sqrt{6}$ (for triangular probability distribution)
$= \sqrt{2}$ (for U-shaped probability distribution)

c_i
Sensitivity coefficient, which is usually estimated from the partial derivatives of the functional relationship between the output quantity (the residual stress) and the input quantities

s
Standard deviation.

A1.5 Numerical Examples

A1.5.1 Surface Residual Stress Measurement

Consider a sample which has a homogeneous stress state across the surface, and the customer would like to know the level of residual stress in the near surface region, with an associated uncertainty. To estimate the uncertainty in the residual stress value measured the user has identified the main contributors to the uncertainty in the measurement. These are:

- Repeatability of the measurement
- Modulus of elasticity
- $\text{Sin}^2\psi$ fit

To evaluate the repeatability of the measurement the user can perform a number of repeat measurements, in this case let us assume the user performs ten repeat measurements where the sample is removed between each test and repositioned in nominally the same location. Thus we have a measure of the combined instrument and operator repeatability. These measurements are presented above in Table A1.1 as series 2. We use the standard deviation between these ten measurements as the value to use in the uncertainty budget.

The customer has not specified the elastic modulus of the material and no extra material has been supplied to measure this value. The operator therefore user has to make an informed estimate as to what value to use for the elastic modulus. Having made this estimate the operator then assumes this value to be within ±5% of the true value. If the customer had specified the elastic modulus value to use, then the contribution to the overall uncertainty can be removed from the uncertainty budget, provided the customer is in agreement.

Finally we need to consider the error in the peak fitting and linear or elliptical curve fitting performed by the analysis software. These errors are usually combined and reported as an error in the stress value by commercial stress packages.

When conducting the final uncertainty calculation it is recommended to construct a table such as that given in Table A1.2, which shows how the uncertainty budget calculations from the above example are calculated.

Table A1.2 - An example of an uncertainty budget worksheet for calculating the uncertainty in residual stress measurement using the XRD method and the data from the series 2 measurements.

Source of uncertainty	Value	Probability Distribution	Divisor d_v	c_i	u_σ MPa ±
Repeatability of measurement (1)	±8.6 MPa	Normal	1	$\frac{s}{\sqrt{n}}$	2.7
Modulus of elasticity (2)	±5%	Rectangular	√3	σ	15.6
$Sin^2\psi$ fit (3)	±27 MPa	Rectangular	√3	1	15.6
Combined standard uncertainty (4)		Normal			22.2
Expanded uncertainty (5)		Normal (k=2)			44.4

Further details of how to determine the type of probabilities and the associated 'divisors' are given in Ref. 8. For this calculation it is sufficient to note that:

(1) This is the combined instrument-operator repeatability, *s,* the standard deviation of all the results calculated from Table A1.1. The corresponding standard uncertainty in σ is, therefore, $u_\sigma = \pm \frac{s}{\sqrt{n}}$, where n is the number of measurements ($u_\sigma = \pm 0.86/\sqrt{10}$).

(2) E was assumed = 210 GPa ± 5 %. The corresponding standard uncertainty in σ is, therefore, $u_\sigma = \pm 0.05 \times 539/\sqrt{3}$.

(3) From Table A1.1.

(4) Combined standard uncertainty, u_c = root sum squares of $u_\sigma = \sqrt{(2.7)^2 + (15.6)^2 + (15.6)^2}$.

(5) Expanded uncertainty, $U = k\, u_c$, where k is a coverage factor = 2 (corresponds to 95% confidence).

The estimated residual stress value in the above example is, therefore, -539 ± 44 MPa.

The above reported expanded uncertainty is based on a standard uncertainty multiplied by a coverage factor k=2, which corresponds to a level of confidence of approximately 95 percent.

A1.5.2 Residual Stress with Respect to Depth Profiling

In this instance consider a sample which has a homogeneous stress state across the surface, but has a stress gradient. The customer would like to know the level of residual stress in the near surface region and at depths of 50, 100 and 150 μm. In addition to the residual stress

values the customer would also like to know the associated uncertainty of the stress value and position. To estimate the uncertainty in the residual stress value measured the user can follow the same process as with the example in section A1.5.1. In this example it is assumed that the uncertainty in the stress value is ±10% of the measured value. This value has been found to be valid for most materials with the equipment used in this example.

The main contributors to the uncertainty in the position of the new surface, if we assume a micrometer has been used are:

- Repeatability of the measurement
- Resolution of the micrometer

To evaluate the repeatability of the measurement the user can perform a number of repeat measurements over the polished region. Not only will this give a measure of the repeatability of the micrometer measurement but will also give an indication of the flatness of the polished region. An example of repeat measurements is shown in Table A1.3.

Table A1.3 Micrometer readings for the new surface position and corresponding residual stress measured at that location.

Position	Micrometer Reading, mm							Residual Stress	Error
	1	2	3	4	5	Average	Std Dev	MPa	±MPa
Surface	4.188	4.192	4.185	4.188	4.195	4.190	0.0040	90	14
Nominally 50 μm	4.139	4.136	4.145	4.147	4.139	4.141	0.0046	70	11
Nominally 100 μm	4.100	4.083	4.084	4.102	4.092	4.092	0.0088	-32	4
Nominally 150 μm	4.050	4.013	4.044	4.034	4.039	4.036	0.0142	-24	11

Having performed the necessary measurements, the uncertainty budget can be constructed, as shown in Table A1.4.

Table A1.4 - An example of an uncertainty budget worksheet for calculating the uncertainty in depth measurement for the surface measurements as shown in Table A1.3.

Source of uncertainty	Value	Probability Distribution	Divisor d_v	c_i	u_σ mm ±
Repeatability of measurement (1)	±0.0040 mm	Rectangular	√3	$\frac{s}{\sqrt{n}}$	0.0010
Resolution of micrometer	±0.01 mm	Rectangular	√3	σ	0.0057
Combined standard uncertainty (2)		Normal			0.0058
Expanded uncertainty (3)		Normal (k=2)			0.0116

Further details of how to determine the type of probabilities and the associated ‘divisors’ are given in Ref. 8. For this calculation it is sufficient to note that:

(1) This is the repeatability of the depth measurement, *s,* the standard deviation of all the results calculated from Table A1.3. The corresponding standard uncertainty in σ is, therefore, $u_\sigma = \pm \frac{s}{\sqrt{n}}$, where n is the number of measurements (u_σ = (±0.0040/√5)/√3).

(2) Combined standard uncertainty, u_c = root sum squares of $u_\sigma = \sqrt{(0.001)^2 + (0.0057)^2}$.

(3) Expanded uncertainty, U = k u_c, where k is a coverage factor = 2 (corresponds to 95% confidence).

The estimated thickness of the sample (i.e. original surface position) in the above example is, therefore, 4.190 ± 0.0116 mm.

The above reported expanded uncertainty is based on a standard uncertainty multiplied by a coverage factor k=2, which corresponds to a level of confidence of approximately 95 percent.

Hence the presented data could resemble that shown in Table A1.5 and Figure A1.1. The uncertainty in the depth position has been calculated following the method used to create Table A1.4. The residual stress uncertainty has been calculated following the method described in Section A1.5.1 and Table A1.2.

The values used for this illustration have been taken from actual experimental data obtained at the National Physical Laboratory as part of MMP8.5 Advanced Techniques for Residual Stress Measurements which was part of the Measurements for Processability and Performance of Materials Programme, a programme of underpinning research funded by the United Kingdom Department of Trade and Industry.

Table A1.5 Example of depth profiling results showing the depth and residual stress measured along the uncertainty in the value for each case.

Position	Depth, μm	Uncertainty in depth, ± μm	Residual Stress, MPa	Uncertainty in residual stress, ± MPa
Surface	0	11.6	90	9
Nominally 50 μm	48.4	11.6	70	7
Nominally 100 μm	97.4	12.3	-32	3.2
Nominally 150 μm	153.6	13.5	-24	2.4

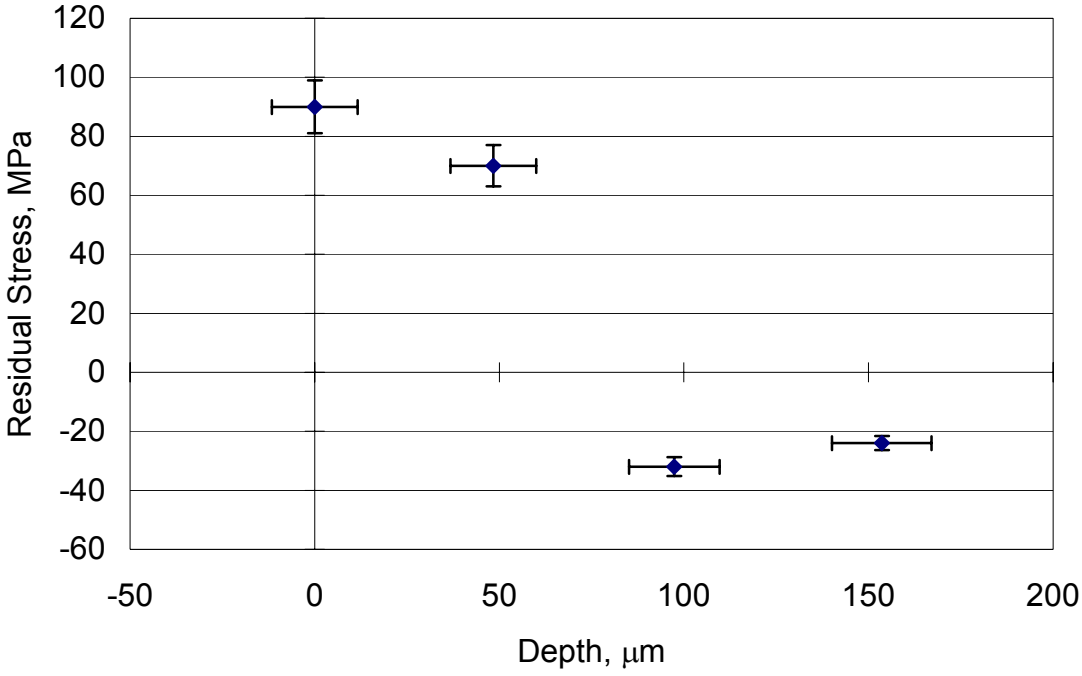

Figure A1.1 Example of data presentation for residual stress depth profile with uncertainty estimates for the stress and depth values.

Appendix II

Options for Data Analysis

One of the most important parts of the X-ray stress measurement procedure is the determination of the diffraction peak position. Software supplied by the equipment manufacturer is generally used to do this, and the exact method of peak fitting and data analysis may well vary depending on the software supplied. In this section a short review of the common methods is given.

Typically, only the shift in the peak position between different ψ - tilts is needed for accurate stress determination. It is not necessary to know the precise diffraction angle, although an approximate knowledge of the 2θ value (to within 1°) is required.

Before the peak position or shift can be determined, the raw intensity data have to be corrected for any effects from Lorentz-polarization factor and variable absorption. This is especially important with broad peaks. The Lorentz-polarization depends on the geometry of the X-ray set-up and the diffracting planes which are used. The absorption correction is needed because the X-ray beam will have a different mean penetration at different angles between the specimen and the incident beam. The correction factors are usually 'hidden' within the analysis software, and may not be needed depending on the geometry of the equipment and the measurement.

It is then recommended that the peak be corrected for asymmetry arising from the presence of the K-α_1 and K-α_2 doublet. In essence, the measured peak consists of two overlapping peaks because of the two energy emissions from the X-ray tube. In most practical cases of stress measurement the splitting of the doublet cannot be seen. In the elimination of the K-α_2 doublet when there is no separation, it has to be assumed that the two components have the same shape, the intensity ratio is known (the α_2 peak is taken to be half the intensity of the α_1 peak) and the spacing of the doublet is known. In most cases the doublet elimination seems to have a minimal effect on the resulting stress value.

There are numerous methods to determine the peak location. These methods can be divided into two groups. The first group are the localized methods, in which only a small portion of the peak is being used. Examples of these methods are the parabolic and half-maximum breadth (H/2) methods (the first and third examples in Figure A2.1). As can be seen, these methods use only a small fraction of the recorded peak to calculate the centroid position. If the whole diffraction peak is available, which is the usual situation with modern diffractometers, there is no need to restrict the data analysis to such a small part of the peak as is the case with these localized methods.

The centre-of-gravity (or centroid) method is the most common traditional method of peak fitting, which uses all information in the diffraction peak. Another common method is the cross-correlation method, which determines the peak shift. Both of these methods are restricted to cases in which the peak is clearly defined. Both are sensitive to truncated peaks, where the full peak profile has not been obtained. A so-called 'sliding' centre of gravity

method has also been developed, which is said to be less sensitive to background subtraction in the case of broad peaks.

One disadvantage of these methods is that they do not give any information about the width of the peak, which is useful in some analyses. That has to be determined separately from the diffraction peak itself. However, both methods are easy and simple to use. Figure A2.1 presents a summary of different peak position determination methods.

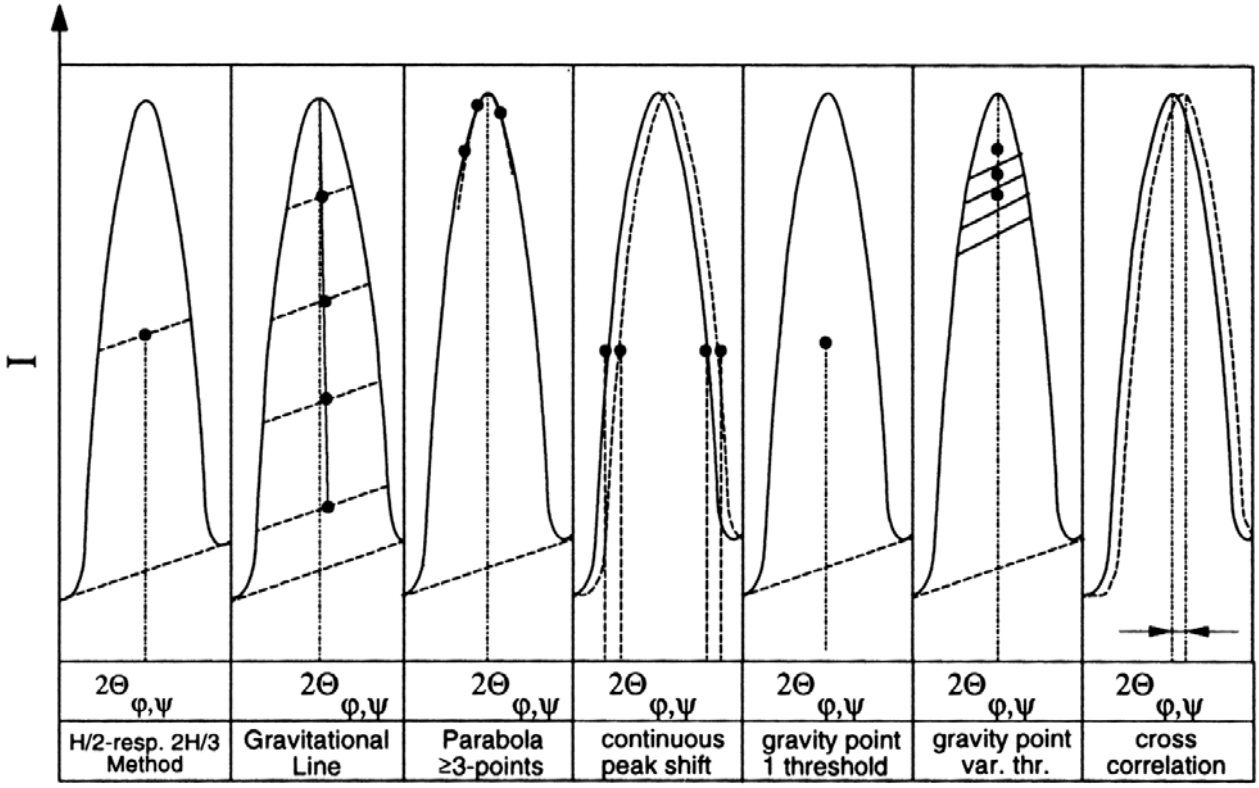

Figure A2.1 Comparison of methods used for peak position determination (After Ref. 5)

The diffraction peak can also be represented by a mathematical function, the most common being Gaussian, Lorentzian, Pearson VII and Voigt or Pseudo-Voigt. All of these represent the same bell shape of a graph with small modifications. None of them can be recommended as the best one for all cases. The first two functions are as follows:

Gaussian

$$I(x) = a_0 \exp\left[-0.5\left[\frac{x - a_1}{a_2} \right]^2 \right] \qquad \textbf{16}$$

Pearson VII

$$I(x) = \frac{a_0}{\left[1 + 4\left(\frac{x - a_1}{a_2}\right)^2 \left(2^{a_3} - 1\right)\right]^{a_3}} \qquad \textbf{17}$$

Where a_0 = Amplitude (I_0)
a_1 = Centre (2θ)
a_2 = Width1
a_3 = Width2

Benefits of fitting the peak profile, rather than using one of the methods shown in figure A2.1 are:

(1) It takes all the data into account
(2) It can handle many partly overlapping peaks
(3) Stripping $K\alpha_{1,2}$ is simplified
(4) Fitting of background can be combined
(5) It directly gives the position of the peak and FWHM.

An example of fitting result is given in Figure A2.2 with K-α_1 and K-α_2 separated.

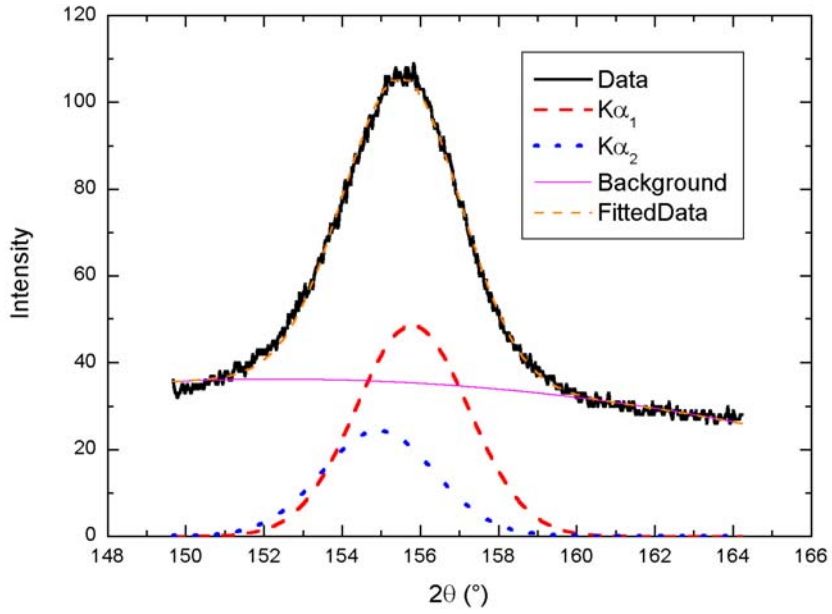

Figure A2.2 Example of fitting a Gauss function to a measured peak, with $K\alpha_{1,2}$ separated and parabolic background

The starting parameters selected for the peak fitting have to be reasonable. Otherwise it is possible that the fitting routine diverges from the measured data, and that the fitted profile does not match the measured peak. It is also typical that the fitting result for the same data can vary slightly depending on the starting values of the parameters.

It is always easier and faster to fit functions that have fewer parameters. Of the functions described above, Gaussian and Lorenzian have three parameters and Pearson VII four. **Also, in general the diffraction peaks are closer to a Gaussian than a Lorentzian shape, which makes the Gaussian function best for standard X-ray stress measurement applications.** The Pearson VII function gives, in some cases, a slightly better match than the Gaussian function, but the difference is small compared to the disadvantage, which is that the function tends to diverge from the data. **With some software packages a general drawback of the fitting procedures is that it is difficult to automate them, which means that they need to be continuously monitored by the user.**

The following factors can particularly affect the quality of data analysis:

- **Large grain size: not enough diffracting grains to give a smooth intensity distribution in the peak.**

- **Texture: the peak can totally disappear in some ±ψ positions.**

- **Too low net intensity: the lower the intensity, the higher the scatter in the results of the peak shift determination. However, there is a limit in increasing the intensity beyond which no further benefit in reduced scatter is obtained.**

- **Superposition of many diffraction peaks: this typically happens when there is more than one phase in the sample.**

- **Distorted diffraction peaks: caused, for example, by a steep stress gradient, or distortion of the crystal lattice (such as cubic distorted to a tetragonal structure typical for hardened steels with a high carbon content).**

- **Truncated broad peaks, where the background is not well defined. This is a typical situation with many position-sensitive detectors, the width of which can be between 10 and 20°. In this case, applying a linear background subtraction causes large errors because the background noise has been incorrectly described.**

In practical measurements it is typical that diffraction peaks are not symmetrical. The effect of the non-symmetrical peaks is in most cases small in standard stress measurement, and the peaks can be treated as symmetrical. Asymmetry is more or less constant as a function of the tilt so the effect on peak shift determination is small.

To conclude, if peaks are clearly separated and the background is well defined, every method works well in the determination of the peak location. In other cases it is recommended to use a proper peak fitting method. The most simple peak fit method is to use a Gaussian function.

These recommendations are meant for stress analysis where only the peak *shift* is determined. If a full triaxial analysis of stress is performed, using a stress-free reference, then the absolute peak location has to be determined and it is crucial that all steps are followed as thoroughly as possible, including the use of procedures which can handle non-symmetrical peaks. **However, such an analysis is beyond the scope of this Guide, which assumes that measurements are made with the assumption that the stress normal to the surface is zero, and so a full triaxial analysis is not required.**

Appendix III

Safety Issues

The safe use of X-ray equipment is the responsibility of the individual, who should follow and abide by international and national legal requirements, such as *The Ionising Radiations Regulations 1999* in the UK; as well as local work rules and procedures in place within their organisations.

WARNING

- **Radiation burns from X-rays are serious injuries. Symptoms are not immediately apparent, except for reddening of the skin.**

- **Such burns must receive immediate medical attention.**

INFORMATION The primary beam from the X-ray tube rapidly causes death of irradiated tissue. When the blood stream takes the toxins (proteins) away from the injury, the blood corpuscles tend to precipitate quicker (due to excess proteins) and cause blockage in fine blood vessels in vital organs and elsewhere. This is similar to a large burn or crush injury. Healed, severe radiation burns leave scar tissue.